+

FFSAR - COASTAL

Fully Focused SAR Altimetry and innovative river level gauges for Coastal Monitoring

Product Validation and Evaluation Report

Deliverable D2.2

Fully Focused SAR Altimetry and innovative river level gauges for Coastal Monitoring

ESA Contract 4000136960/21/I-DT-Ir

Project Reference FFSARCOASTAL_ESA_MTR_D2.2
Issue:2.1

This page has been intentionally left blank

Change Record

Date	Issue	Section	Page	Comment
21/09/2022	1.0	all	all	1st version
06/07/2023	2.0	all	all	2nd version
22/08/23	2.1	various	various	updates following ESA review

Control Document

Process	Name	Date
Written by:	Heidi Ranndal Mikkel Aaby Kruse	21/09/2022 06/07/2023
Checked by	David Cotton	
Approved by:		

Subject	Fully Focused SAR Altimetry and Innovative River Level Gauges for Coastal Monitoring	Project	FFSARCOASTAL
Author	**Organisation**	**Internal references**	
Heidi Ranndal, Karina Nielsen, Mikkel Aaby Kruse, Ole Baltazar Andersen	DTU	FFSARCOASTAL_ESA_MTR_D2.2	

	Signature	Date
For FFSARCOASTAL team	David Cotton	23/08/23
For ESA		

Table of Contents

1 Introduction

1.1 The FFSAR Coastal Project

In this project, the Fully Focussed (FF) SAR altimetry processor was applied on Sentinel-3 and its potential to make a significant new contribution to coastal and estuarine monitoring systems was validated using innovative water level gauges.

Here the focus was on applications that benefit from the high along-track resolution in water level provided through Fully Focussed SAR processing. The FFSAR processing was conducted for three Sentinel-3 tracks in the two study regions: The Severn Estuary in the UK and the Rhône River in France. User agencies and groups from the two regions were consulted to identify gaps and priorities for monitoring requirements.

Innovative in-situ water level gauges are used to validate the satellite-based water levels. Time series is provided by autonomous gauges placed at fixed locations, gauges mounted on drones were used to provide water level profiles between the fixed locations and satellite tracks.

1.2 Scope of this Document

The purpose of this document is to present the validation and evaluation of the FFSAR-processed Sentinel-3 data carried out by DTU for the ESA FFSAR-Coastal project. The validation and evaluations are carried out for both study regions, the Severn Estuary and the Rhône River.
We have included in two annexes additional work carried out by NOC (Validation of vortex.io microgauge data against other gauge data: Newport and Weston Super Mare) and SatOC (Comparison of drone data to Newport harbour TG data)

1.3 Applicable Documents

AD-01: Fully Focussed Sar Altimetry And Innovative River Level Gauges For Coastal Monitoring (FFSAR-Coastal) - ESA Contract No. 4000136960/21/I-DT-Ir

1.4 Reference Documents

RD-01 FFSAR-Coastal Proposal. V1.1 29/07/21, SatOC and FFSAR-Coastal team.

1.5 Overview of this Document

This deliverable is organised into the following sections:

Section 2: The study areas
Section 3: FF-SAR Sentinel-3 data
Section 4: Validation data
Section 5: Evaluation and discussion

Annex 1: Validation of vortex.io microgauge data against other gauge data: Newport and Weston Super Mare
Annex 2: Comparison of drone data to Newport harbour TG data

2 Study areas

This section briefly introduces the two study areas and gives an overview of the geographic pavement of the analysed Sentinel-3A (S3A) and Sentinel-3B (S3B) satellite tracks.

2.1 Severn Estuary, England

The Severn Estuary is the inner part of the Bristol Channel. This area is subjected to extremely strong diurnal tides (ranging up to 15m), which makes it a very interesting place for hydrological and flood modelling. Concerning altimetry, the Severn Estuary is a very challenging area because of the severe snagging that occurs due to extremely specular targets off-nadir. Many S3A and S3B reference ground tracks cross the estuary, but six tracks in particular provide data for the area east of Swansea in Wales, which is the region of interest for this analysis. The study area along with the six reference ground tracks crossing the Severn Estuary can be seen illustrated in Figure 1.

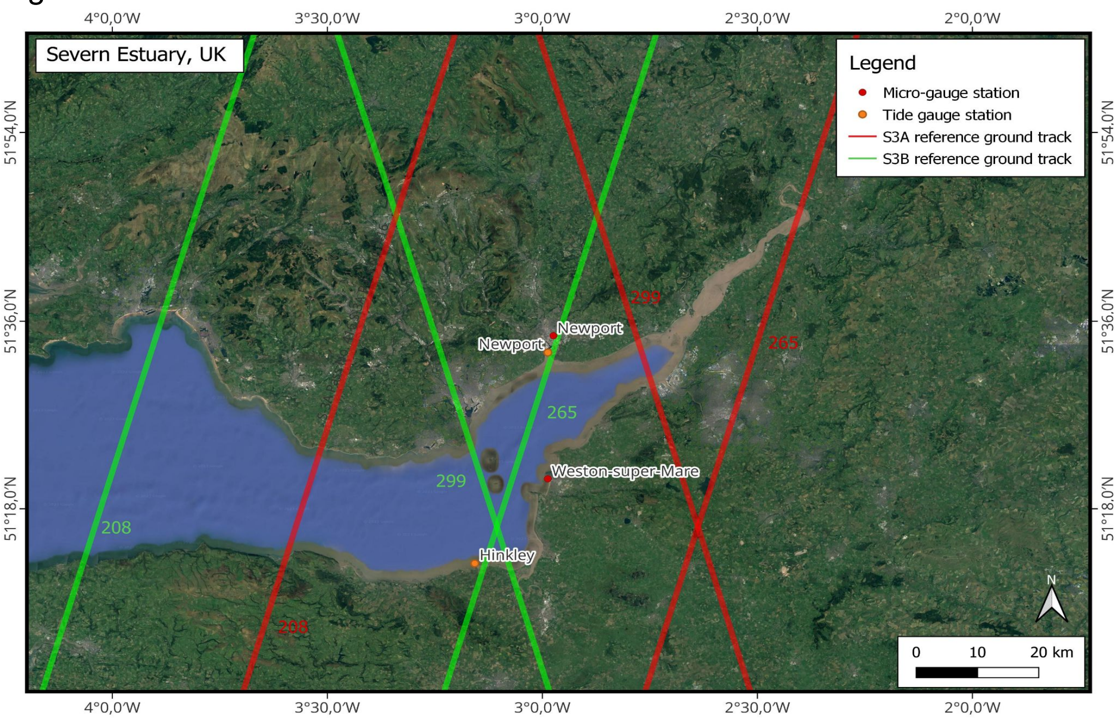

Figure 1: A map showing the Severn Estuary along with the S3A and S3B reference ground tracks that FFSAR altimetry processing was applied to in the presented analysis. The locations of the micro-gauge stations installed by vorteX-io and the two tide gauge stations used in the presented analysis are marked as red and orange dots respectively. [Imagery © TerraMetrics 2023, Map data © 2023 Google]

2.2 Rhône River, France

The Rhône River in France is a low-lying river in a delta consisting of wetlands. The river is quite narrow (approximately a width of 400 m in the study area), and therefore the usual 20 Hz processing of the Sentinel-3 data would only provide a few or a single water level estimate. Using a high posting rate from FFSAR, obtaining a high number of water level estimates is possible. The heterogeneity of the area leads to very contaminated waveforms and is therefore a difficult area to obtain a stable water level in. For the area of the Rhône River investigated in this project, only the tracks with RONs 179 and 199 from S3B are of interest. Track S3B-179 crosses the inner harbour area and a small manmade canal (width of approximately 60 m) where the micro-gauge is installed and track S3B-199 crosses the river at three locations. Both reference ground tracks in the study area can be seen as illustrated in Figure 2.

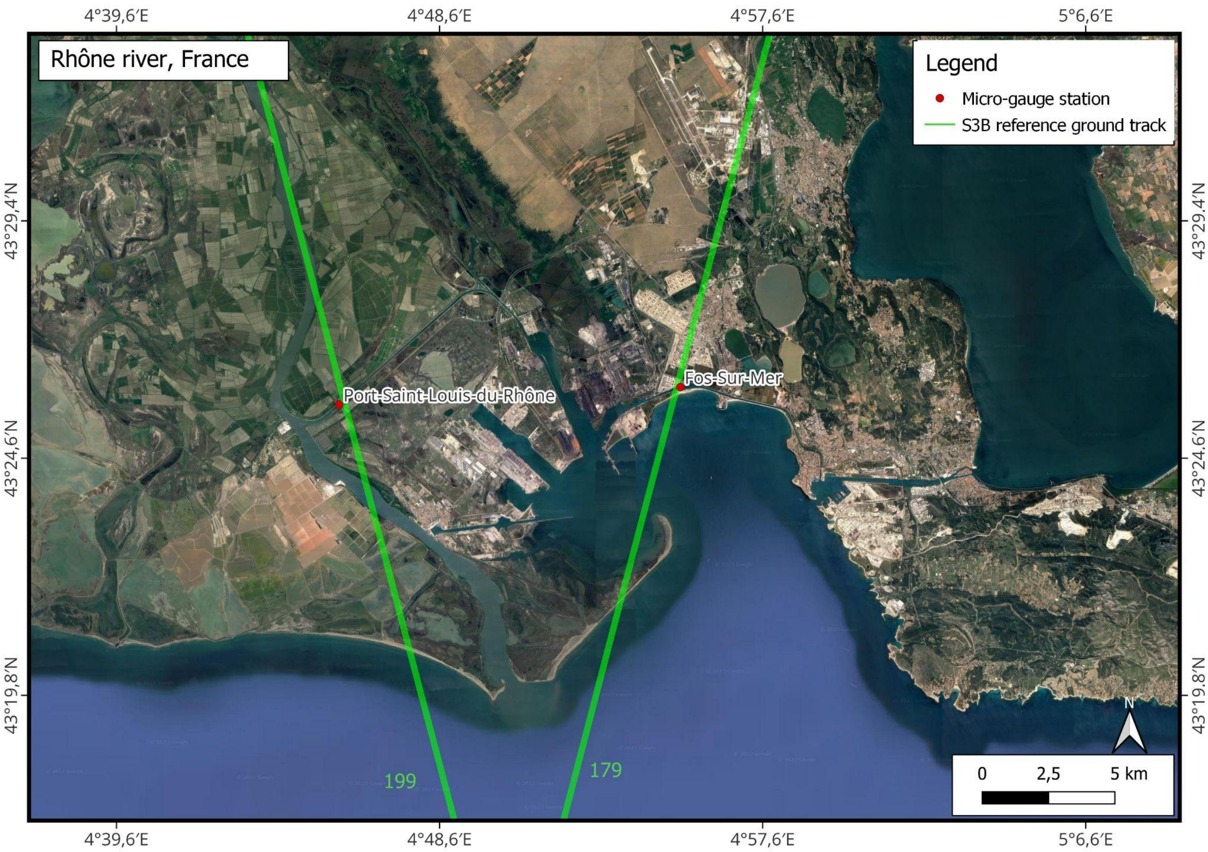

Figure 2: A map of the Rhône River along with the S3B reference ground tracks that FFSAR altimetry processing was applied to in the presented analysis. The locations of the two micro-gauge stations installed by vorteX-io are also shown as red dots. [Imagery © TerraMetrics 2023, Map data © 2023 Google]

3 FFSAR Sentinel-3 data

3.1 FFSAR data in the Severn Estuary

The analysis of the Severn Estuary initially included data from all six reference ground tracks illustrated in Figure 1. As the project progressed, time constraints necessitated a decrease in the scope of the analysis to carry out a meaningful validation. As only the track with RON 265 from S3B intersects the location of any of the vorteX-io micro-gauge stations, the analysis was refocused on this specific reference ground track. While data from all six tracks were downloaded and processed using SMAP, only data from track S3B-265 was validated and analysed in detail. Validation of the remaining five tracks would be possible in a follow-up activity but is beyond the scope of the work presented here. All downloaded data for the Severn Estuary were processed using a posting rate of 1000Hz and are summarized in Table 1.

RON	Sentinel-3A period (cycles)	Sentinel-3B period (cycles)
265	Apr 2016 (cycle 3) – May 2022 (cycle 85)	**Dec 2018 (cycle 19) -April 2023 (cycle 78)**
299	Apr 2016 (cycle 3) – May 2022 (cycle 85)	Feb 2018 (cycle 21) – June 2022 (cycle 66)
208	May 2016 (cycle 4) – June 2022 (cycle 86)	Dec-2018 (cycle 19) – June 2022 (cycle 66)

Table 1: Downloaded and processed data for S3A and S3B in the Severn Estuary. The data series highlighted in bold letters originate from the specified reference ground track in focus. RON = Relative Orbit Number.

3.2 FFSAR data in the Rhône River

For the Rhône River two tracks are relevant for this project, namely the tracks with RONs 179 and 199 from S3B. 179 is a descending track, and 199 is ascending. Both RONs have been downloaded and processed using a posting rate of 1000Hz. Due to the characteristics of this region, the SMAP was run using posting rates in the range of 500Hz to 1500Hz with 100 Hz intervals for both tracks. All downloaded and processed data from these two tracks are summarised in Table 2.

RON	Sentinel-3B period (cycles)
179	**March 2019 (cycle 23) – April 2023 (cycle 78)**
199	**Dec 2018 (cycle 19) – May 2023 (cycle 79)**

Table 2: Downloaded and processed data for S3B in the Rhône River, France. The data series highlighted in bold letters originate from the specified reference ground track in focus. RON = Relative Orbit Number.

4 Validation data

This section describes the different validation data available for the two study regions.

Originally a further validation in the Severn Estuary had been planned using NW European shelf model output, using FFSAR processed data from passes further to the west (e.g., S3A and S3B passes 208 in figure 1.) However, data from these tracks was not processed with the FFSAR processor, as effort was instead focussed on implementing the MWaPP re-tracker and validating against ICESAT-2 data. Consequently, this planned aspect of the proposal was not carried out.

4.1 Severn Estuary

This section describes the validation data for the Severn Estuary. Although drone data were available, they were not used as part of the validation.

4.1.1 Drone data (vorteX-io)

Drone-based water levels for the Severn River were collected on 24/2 2023 as an under-flight to track S3B-265. The primary objectives for the drone flights were to provide geo-referencing for the vortex.io microgauge data (the drone flights were themselves geo-referenced to a GNSS ground station), and to provide a continuous water level profile between the vortex.io microgauge locations and the satellite ground-track at the time of the satellite overpass.

4.1.2 Micro-stations (vorteX-io)

Micro-stations have been installed at positions shown in Figure 1. Data is available from September 6th, 2022, and provided as elevation with respect to WGS84 as a function of UTC time.

4.1.3 Tide gauges

Tide gauge data from the Newport and Hinkley tide gauges (see Figure 1) managed by the National Oceanography Centre (NOC) and distributed by the British Oceanographic Data Centre (BODC) provide elevation data in the Admiralty Chart Datum (ACD). Data from these tide gauges has been post-processed and utilised in the ESA HYDROCOASTAL project to validate the performance of improved SAR processing methods (A. Shaw, 2023). The data spans from 01/01/2018 to 17-10-2022 and contains water heights relative to the ACD within a +- 3 std range of the mean water level measured at a given gauge. The tide gauge data was provided by A. Shaw in a personal communication and contains water heights relative to the ACD within a +- 3 std range of the mean water level measured at a given gauge from 01/01/2018 to 17/10/2022. The data have been re-projected to be given with respect to the ETRS89 ellipsoid by adding the local offset between the Ordnance Datum Newlyn (UK mainland) and the ETRS89 reference ellipsoid at the locations of the two tide gauges.

Data obtained from the Hinkley tide gauge from 2021 onwards show signs of instrument failure and were removed.

4.1.4 ICESat-2

The ICESat-2 ATL-13-based water levels [WGS84] were used to constrain the FFSAR altimetry-based water levels.

4.2 Rhône River

This section describes the validation data for the Rhône River. Although drone data were available, they were not used as part of the validation.

4.2.1 Drone data (vorteX-io)

Drone-based water levels for the Rhône River were collected on 13/4 2023 as an under-flight to tracks S3B-179 and S3B-199

4.2.2 Micro-stations (vorteX-io)

Micro-stations have been installed at positions shown in Figure 2. Data is available from July 27th, 2022. The data is provided as elevation with respect to the WGS84 as a function of UTC time.

5 Evaluation and discussion

This section gives an overview of the validation studies and evaluates the quality of the FFSAR data. The main source of data for validation is the VorteX-io micro-gauge stations. ICESat-2 was used to constrain the FFSAR-based water level and a visual inspection of the water slope was evaluated using the drone data collected by VorteX-io qualitative. Additionally, water levels derived from the standard 20Hz OCOG re-tracker were validated with the gauge data to demonstrate the potential FFSAR. The statistical measurements of RMSE and Correlation were chosen as the main properties on which the validation would be based, and a detailed list of the validations conducted for the two study areas is listed in Table 3.
In addition to the RMSE statistic, a Corrected RMSE (RMSE Cor) statistic is also computed. These values are RMSE estimates computed from height values that have had a “Median bias” correction applied to them. This means that micro-gauge height values have been realigned with estimated water surface heights from the different re-trackers to make it easier to judge their ability to follow the change in the dynamic water surface height signal. All standard RMSE values are thus computed from unadjusted time series data.

Severn S3B-265	Rhône S3B-179/S3B-199
Validation of water level for the re-trackers: MWaPP, Multi-PTR, PTR, and OCOG	Validation of water level for the re-trackers: MWaPP, Multi-PTR, PTR, and OCOG
Validation of 20 Hz OCOG water levels	Validation of 20 Hz OCOG water levels
	Validation of FFSAR (500-1500Hz) MWaPP water levels
Visual drone comparison of water slope	Visual drone comparison of water slope
	FFSAR and 20Hz track comparison

Table 3: A table summarising the different validation analyses performed for the two study areas. The Rhône River has been most thoroughly analysed since it contained a greater number of smaller channels with relatively calm waters, thus making it a good candidate for testing the limits of achievable FFSAR results.

5.1 Rhone: Fos-sur-mer

This section presents the validation results for track S3B-179 crossing the industrial harbour in Fos-Sur-Mer. This scene can be subdivided into two separate water bodies of interest shown in Figure 3, an inner harbour area and a narrow canal.

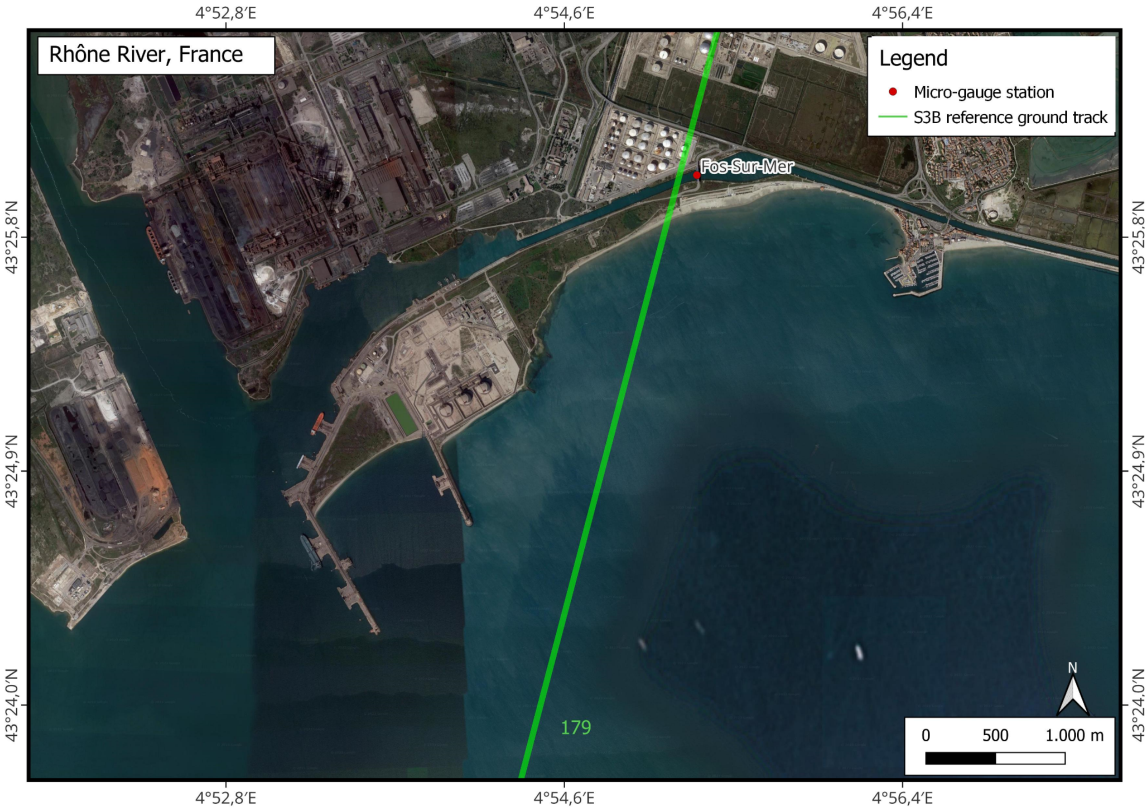

Figure 3: A map showing the location of reference ground track S3B-179 close to the mouth of the Rhône River in Fos-Sur-Mer. The location of the micro-gauge station installed in the small manmade channel by vorteX-io is also shown as a red dot. [Imagery © 2023 Aerodata International Surveys, CNES / Airbus, Landsat / Copernicus, Maxar Technologies, Map data © 2023 Google]

5.1.1 Posting rate validation

Table 4 and Table 5 present the validation results using a range of different posting rates between 500Hz and 1500Hz, and an illumination time of 2.3s and 1s respectively. All water heights used in the computation of these results have been estimated using the MWaPP re-tracker. The time series for each set of tests are also illustrated in Figure 4 and Figure 5. In general, all the results are quite similar for both sets of tests since the target is narrow (~60 m). The data obtained using a posting rate lower than 1000Hz had fewer valid water levels available in the period with available micro-gauge data, and thus their time series also has fewer data points. The best correlation and the lowest RMSE were obtained when using a posting rate of 700, and the highest number of matching heights estimate and micro-gauge reference data was obtained using a posting rate of 1100Hz.

Rhône: Fos-sur-mer Canal, Illumination time: 2.3s

Posting rate [Hz]	Median bias [m]	RMSE [m]	RMSE cor [m]	Correlation	#pair
500	0.41	0.42	0.051	0.90	8
600	0.44	0.45	0.076	0.86	9
700	0.41	0.41	0.033	0.96	8
800	0.40	0.41	0.060	0.84	9
900	0.41	0.42	0.065	0.83	9
1000	0.40	0.42	0.083	0.83	9
1100	0.41	0.44	0.078	0.88	11
1200	0.43	0.46	0.09	0.87	9
1300	0.43	0.44	0.081	0.84	10
1400	0.41	0.43	0.082	0.85	10
1500	0.41	0.42	0.062	0.88	9

Table 4: Summary statistics of the 2.3s illumination time Hz validation test in the manmade canal in Fos-Sur-Mer.

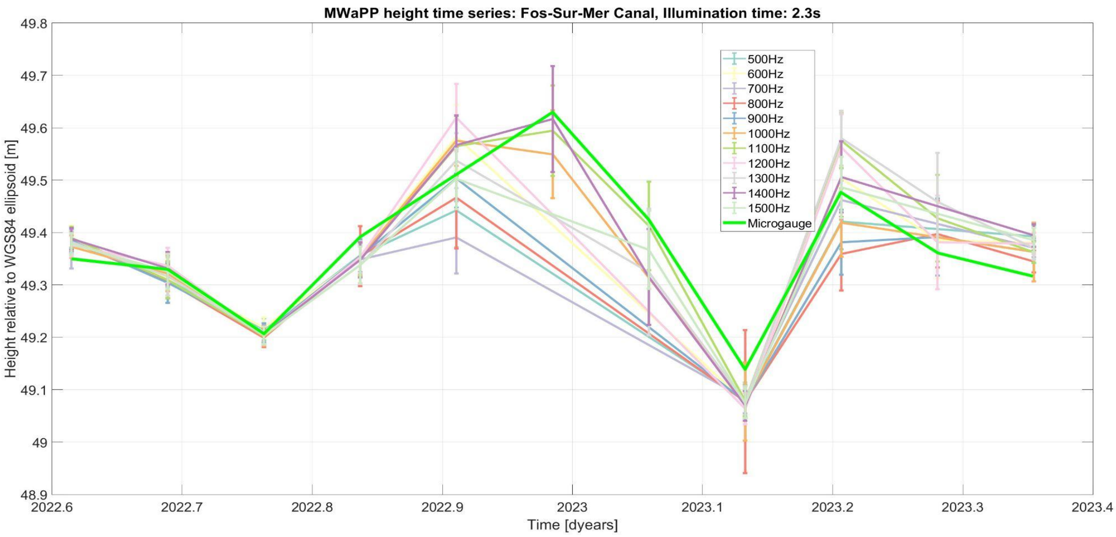

Figure 4: Time series sampled from height estimates obtained using different posting rates between 500Hz and 1500Hz and a 2.3s illumination time in the Fos-Sur-Mer canal. The plotted micro-gauge estimates have been re-aligned to coincide with the time series as a group, by adding the median value of all values in the "Median Bias" column in Table 4.

Rhône: Fos-sur-mer Canal, Illumination time: 1s

Posting rate [Hz]	Median bias [m]	RMSE [m]	RMSE Cor [m]	Correlation	#pair
500	0.40	0.41	0.047	0.91	8
600	0.42	0.44	0.075	0.87	9
700	0.41	0.40	0.034	0.95	8
800	0.40	0.40	0.038	0.93	9
900	0.40	0.39	0.059	0.81	10
1000	0.39	0.41	0.078	0.84	10
1100	0.39	0.42	0.072	0.86	11
1200	0.41	0.44	0.086	0.86	10
1300	0.41	0.43	0.066	0.89	11
1400	0.39	0.41	0.083	0.82	10
1500	0.41	0.40	0.070	0.79	9

Table 5: Summary statistics of the 1s illumination time Hz validation test in the manmade canal in Fos-Sur-Mer.

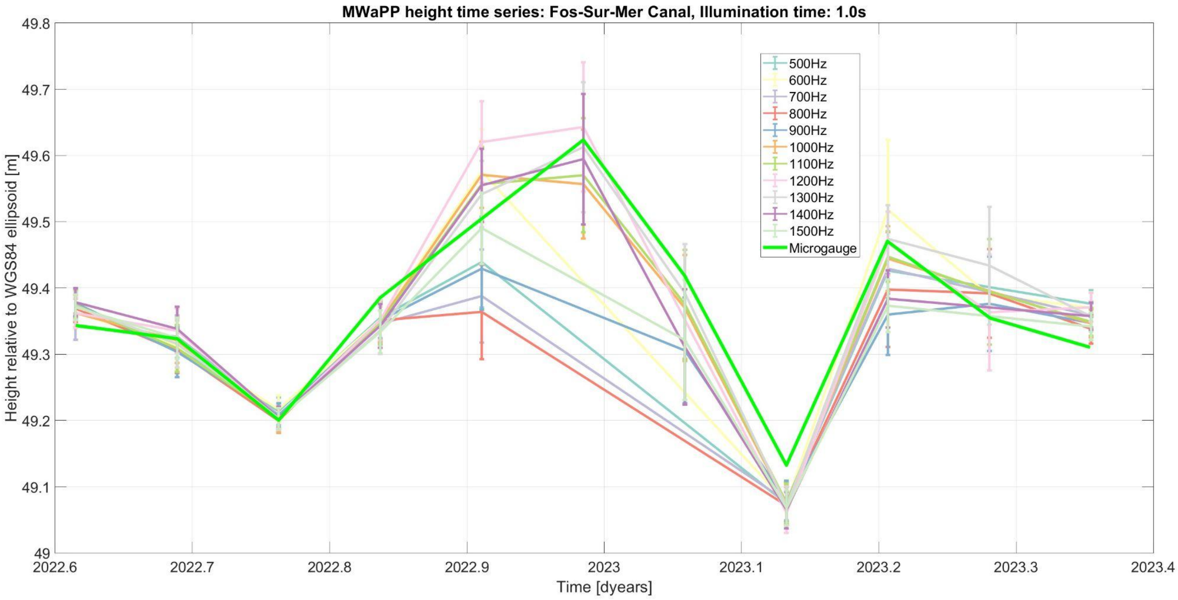

Figure 5: Time series sampled from height estimates obtained using different posting rates between 500Hz and 1500Hz and a 1s illumination time in the Fos-Sur-Mer canal. The plotted micro-gauge estimates have been re-aligned to coincide with the time series as a group, by adding the median value of all values in the "Median Bias" column in Table 5.

5.1.2 FFSAR re-tracker validation

In this section, the FFSAR water levels derived from different re-trackers with a posting rate of 1000 Hz are evaluated.

Figures 6,8,10 and 12 show the FFSAR water levels as a function of latitude processed with the PTR, Multi-PTR, OCOG, and MWaPP re-trackers, respectively. The blue colour represents the measurements from the open harbour area, while the red colour represents the measurements obtained from the canal, the black points represent ICESat-2 measurements from the area, and the green point with the error bar represents the water level range of the gauge station.

Figures 7, 9, 11, and 13 display the estimated water level time series for the two water bodies the canal (red) and the harbour area (blue). The water level as observed by the micro-gauge stations has been plotted as a time series along with these (green) and has been re-aligned with the re-tracker estimates by adding the median bias between the respective time series data and micro-gauge data points. The equivalent time series based on the standard 20 Hz (OCOG) is shown in Figure 12. The summary statistics, RMSE, and Correlation are reported in Table 5.

PTR re-tracker

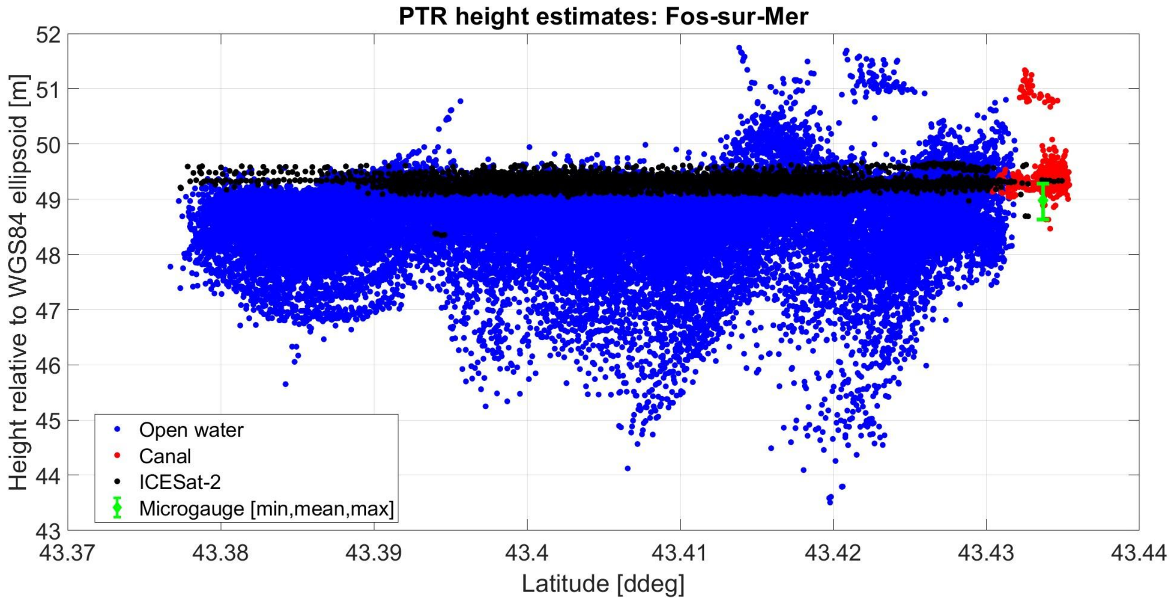

Figure 6: FFSAR water levels estimated by the PTR re-tracker as a function of latitude. The water levels are temporally dispersed throughout the period of analysis highlighted in Table 2 RON 179. The blue data points originate from the open water harbour area of Fos-Sur-Mer. The red data points originate from the manmade canal in Fos-Sur-Mer. The black data points are ICESat-2 data with the same spatial and temporal origin as the input data processed by the re-tracker. The green error bar represents the variance in the observed micro-gauge signal, with the minimum, median and maximum values defining a reference interval.

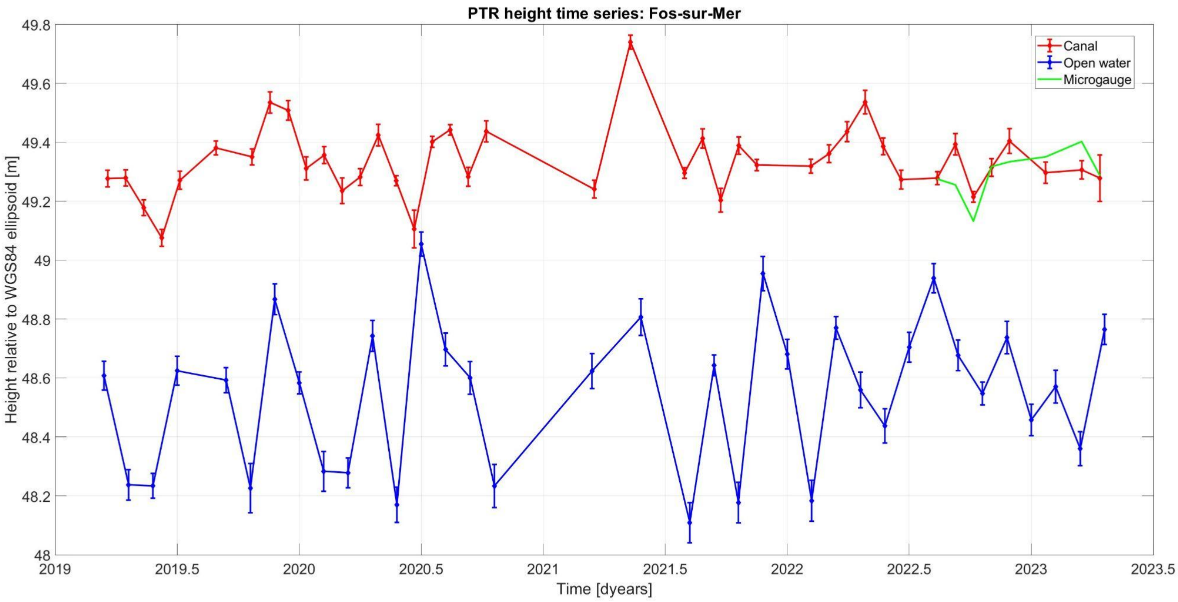

Figure 7: Time series of FFSAR water levels estimated by the PTR re-tracker. The blue and red lines show the dynamic signal of the water levels in the open water and canal areas of Fos-Sur-Mer respectively. The green line shows the dynamic signal of the water level as measured by the micro-gauge.

MultiPTR re-tracker

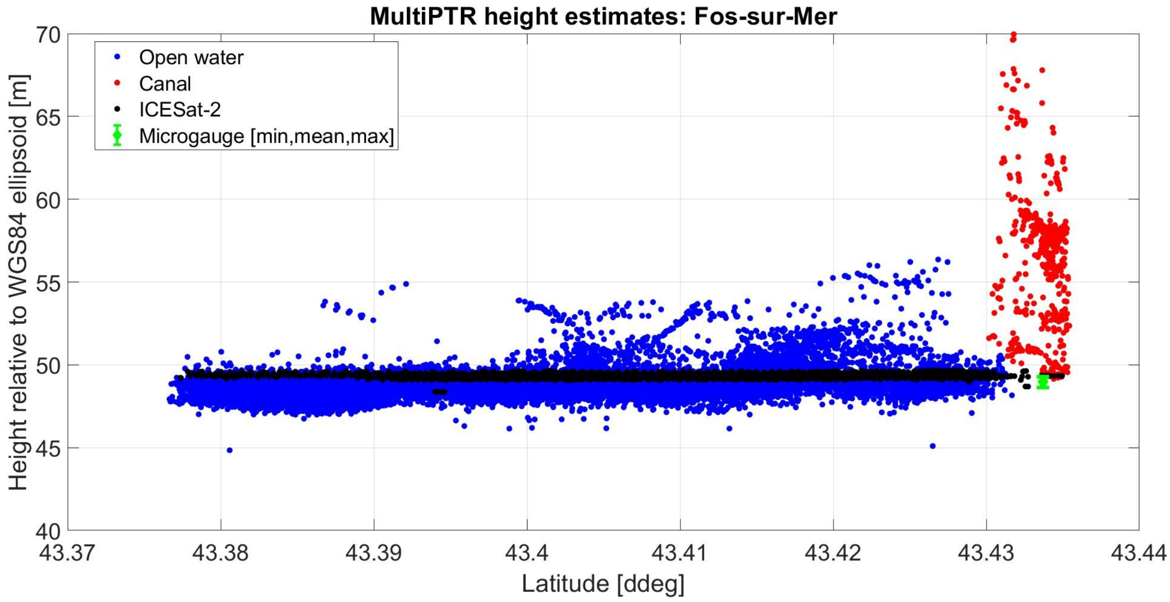

Figure 8: FFSAR water levels estimated by the MultiPTR re-tracker as a function of latitude. The water levels are temporally dispersed throughout the period of analysis highlighted in Table 2 RON 179. The blue data points originate from the open water harbour area of Fos-Sur-Mer. The red data points originate from the manmade canal in Fos-Sur-Mer. The black data points are ICESat-2 data with the same spatial and temporal origin as the input data processed by the re-tracker. The green error bar represents the variance in the observed micro-gauge signal, with the minimum, median and maximum values defining a reference interval.

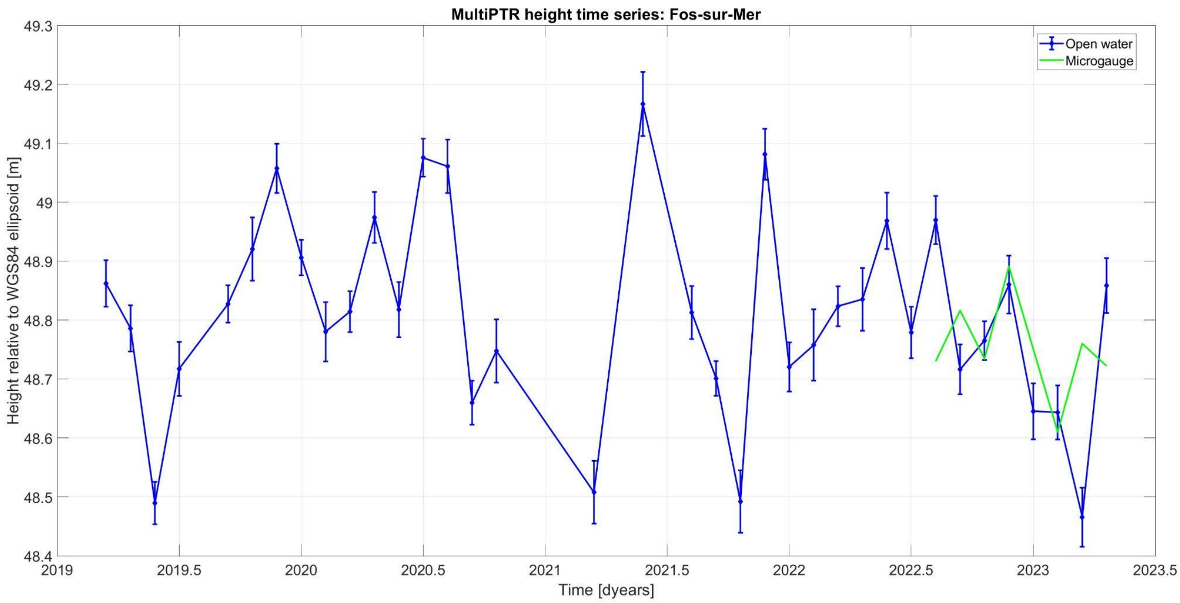

Figure 9: Time series of FFSAR water levels estimated by the MultiPTR re-tracker. The blue line shows the dynamic signal of the water levels in the open water area of Fos-Sur-Mer. The green line shows the dynamic signal of the water level in the canal as measured by the micro-gauge. The MultiPTR re-tracker was systematically incapable of estimating the water level in the canal area correctly, and thus no time series for the canal was produced for this area.

OCOG re-tracker

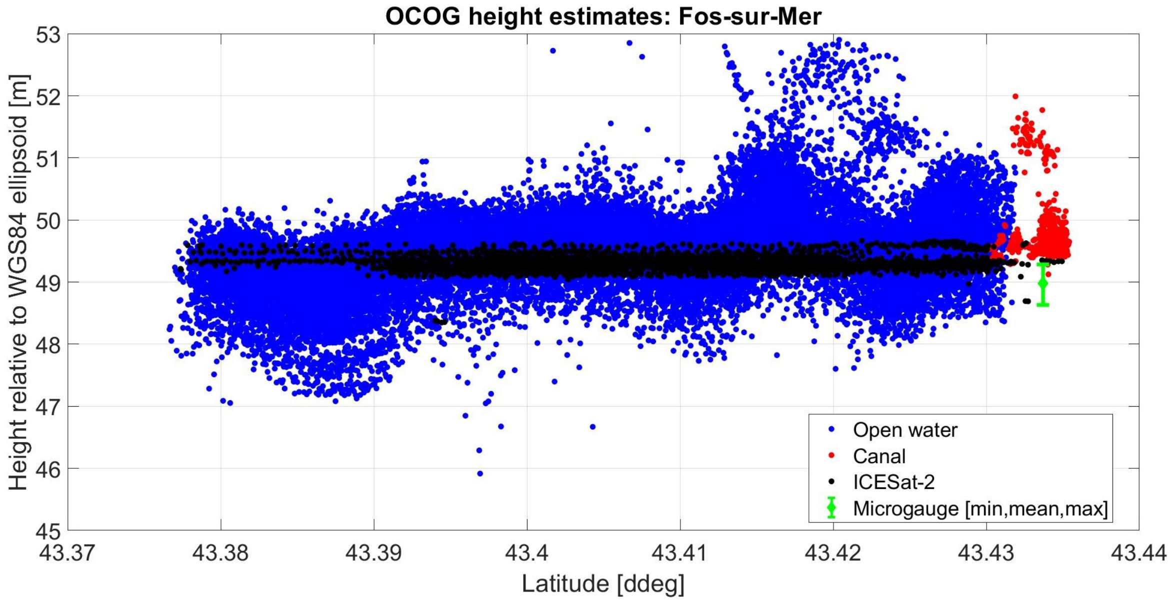

Figure 10: FFSAR water levels estimated by the OCOG re-tracker as a function of latitude. The water levels are temporally dispersed throughout the period of analysis highlighted in Table 2 RON 179. The blue data points originate from the open water harbour area of Fos-Sur-Mer. The red data points originate from the manmade canal in Fos-Sur-Mer. The black data points are ICESat-2 data with the same spatial and temporal origin as the input data processed by the re-tracker. The green error bar represents the variance in the observed micro-gauge signal, with the minimum, median and maximum values defining a reference interval.

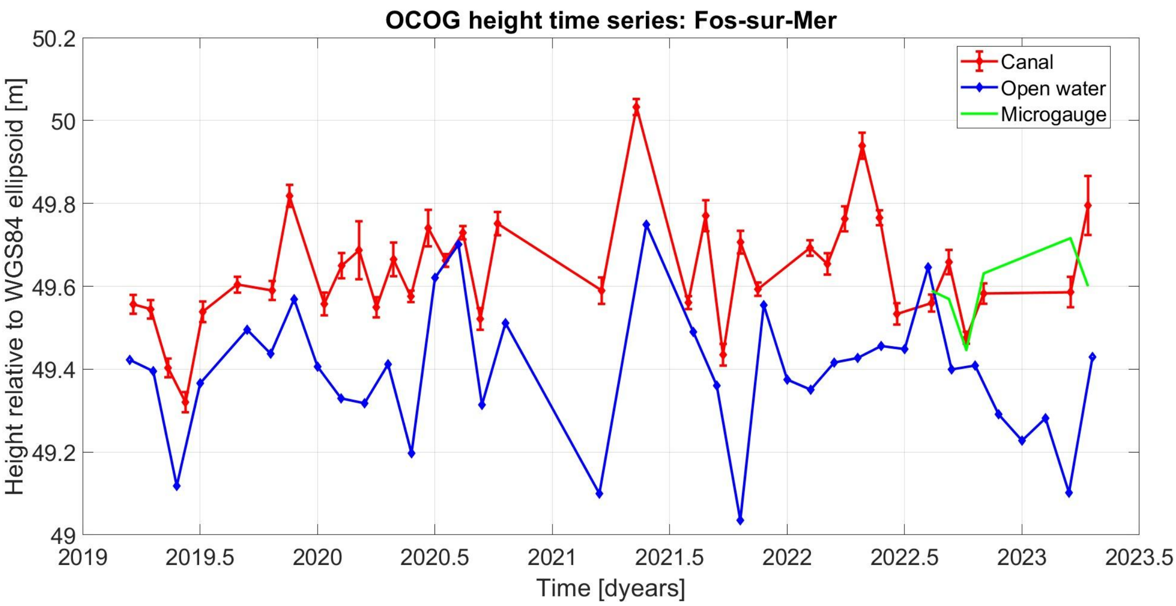

Figure 11: Time series of FFSAR water levels estimated by the OCOG re-tracker. The blue and red lines show the dynamic signal of the water levels in the open water and canal areas of Fos-Sur-Mer respectively. The green line shows the dynamic signal of the water level as measured by the micro-gauge.

MwaPP re-tracker

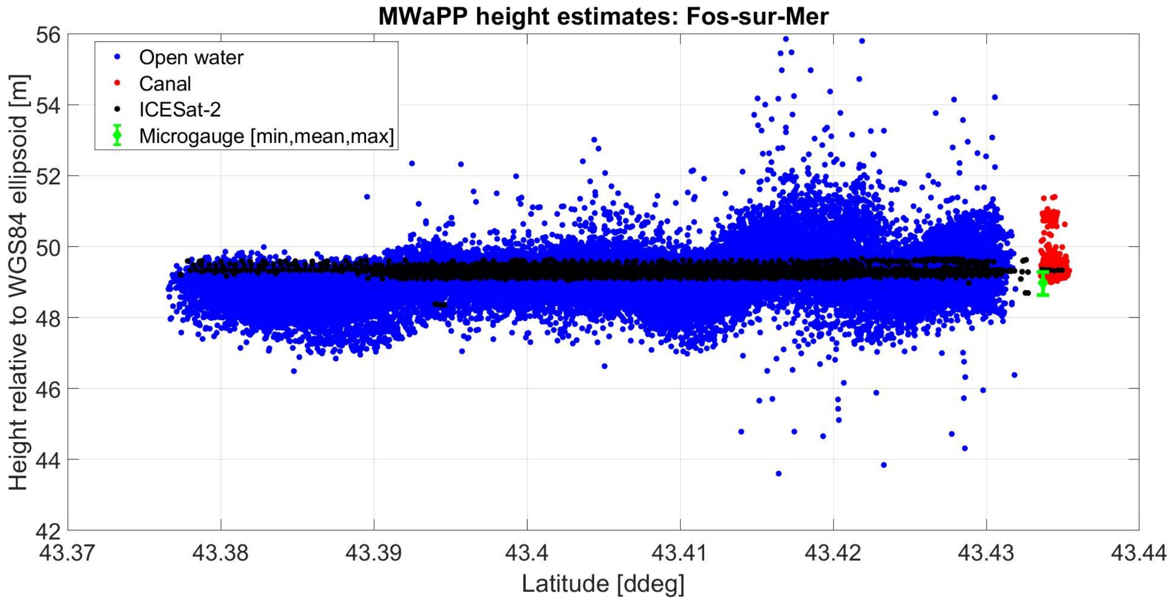

Figure 12: FFSAR water levels estimated by the MWaPP re-tracker as a function of latitude. The water levels are temporally dispersed throughout the period of analysis highlighted in Table 2 RON 179. The blue data points originate from the open water harbour area of Fos-Sur-Mer. The red data points originate from the manmade canal in Fos-Sur-Mer. The black data points are ICESat-2 data with the same spatial and temporal origin as the input data processed by the re-tracker. The green error bar represents the variance in the observed micro-gauge signal, with the minimum, median and maximum values defining a reference interval.

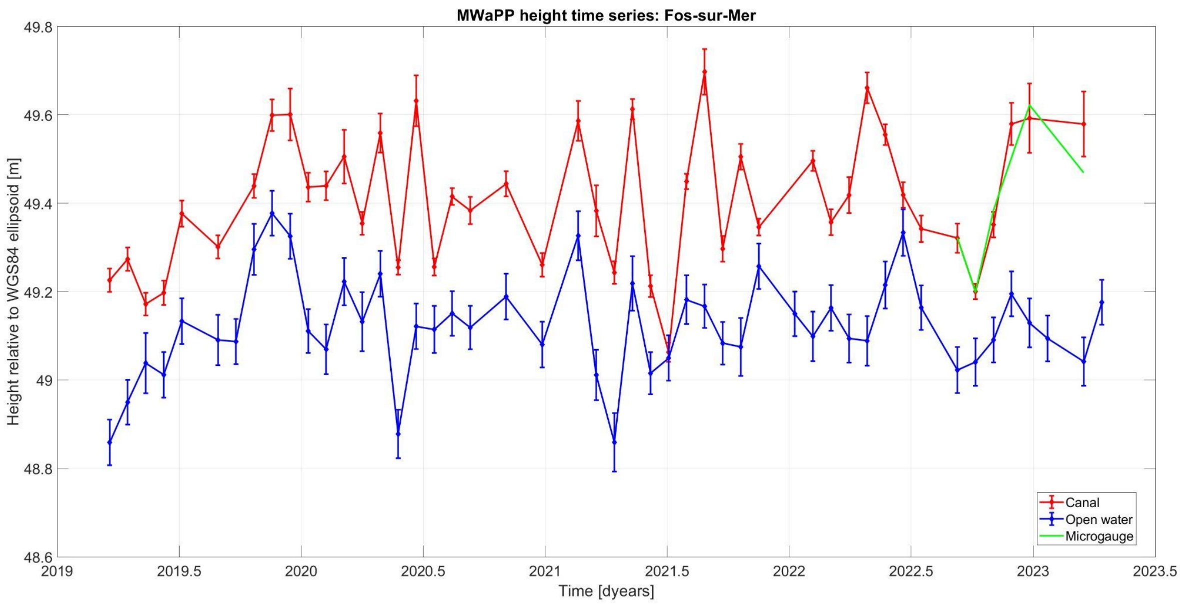

Figure 13: Time series of FFSAR water levels estimated by the MWaPP re-tracker. The blue and red lines show the dynamic signal of the water levels in the open water and canal areas of Fos-Sur-Mer respectively. The green line shows the dynamic signal of the water level as measured by the micro-gauge.

ESA 20Hz OCOG re-tracker

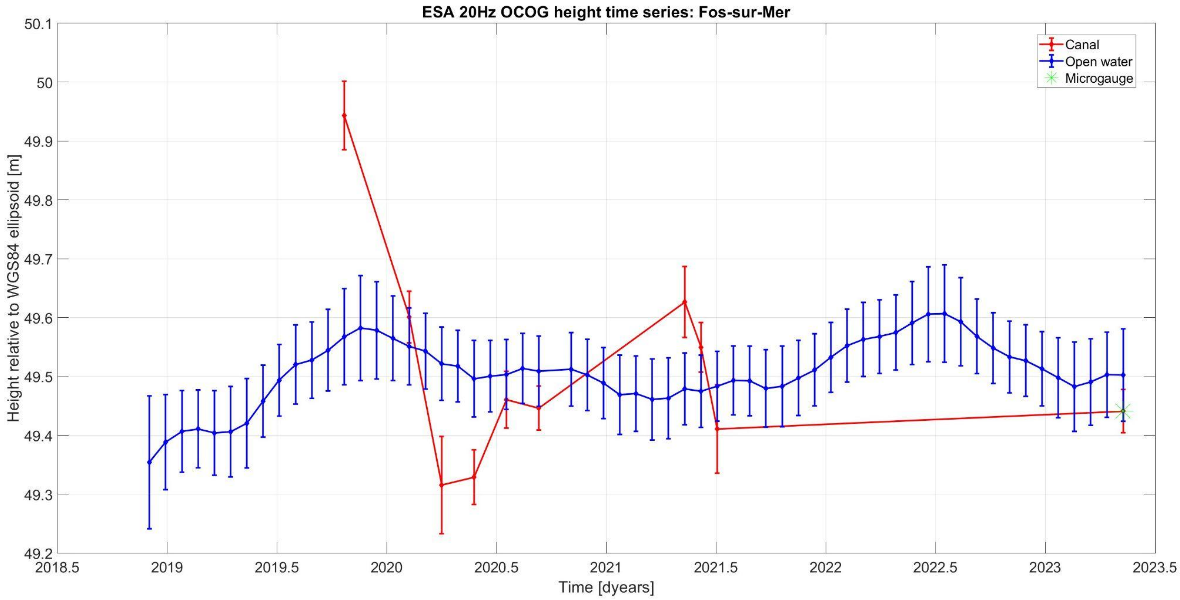

Figure 14: Time series of water levels estimated by the standard 20Hz OCOG re-tracker. The blue and red lines show the dynamic signal of the water levels in the open water and canal areas of Fos-Sur-Mer respectively. The 20Hz OCOG re-tracker is not able to detect the narrow manmade canal reliably in the period with available micro-gauge data, and thus only a single micro-gauge height value is plotted as a green X.

5.1.3 Summary of findings for Fos-Sur-Mer

The resulting height estimates from the employed re-trackers all follow the trend in the change of water level observed by the micro-gauge to varying degrees. A set of summary statistics for the various re-trackers can be seen in Table 6.

Retracker	Median bias [m]	RMSE [m]	RMSE Cor [m]	Correlation
PTR	0.337	0.360	0.073	0.450
MultiPTR	-		-	-
OCOG	0.650	0.675	0.105	0.337
MWaPP	0.403	0.427	0.058	0.939
20Hz OCOG	-	-	-	-

Table 6: Summary statistics for the individual re-trackers. The MultiPTR and 20HZ OCOG re-trackers were both incapable of detecting and or measuring the canal water surface level heights reliably and thus no meaningful statistical computations could be made for their output data.

From Table 6 it becomes evident that the MWaPP re-tracker has both the lowest RMSE and highest correlation with the reference micro-gauge data. This fact is illustrated when analysing the time series in Figure 13. The results obtained in the

Fos-Sur-Mer canal follow the dynamic signal observed in the canal by the micro-gauge station very well. The time series illustrated in Figures 7 and 11 follow the trend observed by the micro-gauge station for the first part of the overlapping measurement periods but deviate noticeably in the later part of the measurement period.

As illustrated in Figure 8, the MultiPTR re-tracker was systematically incapable of estimating the water level in the canal area correctly. The spread in the estimates over the canal (~20m) is larger than the spread in the entire data sets obtained using the other re-trackers and are thus deemed to not originate from within the canal. The spread of the measurements from the open harbour area is approximately 2-3 m with increased snagging towards the coast. Fos-Sur-Mer is a very complex scene containing an industrial harbour with many metallic surfaces and possible corner reflectors, as well as many other disconnected and relatively still-standing water bodies.

The MultiPTR re-tracker may have an inherent weakness when re-tracking waveforms originating from such complex and inhomogeneous scenes. Regardless of the underlying cause, the unrealistic height estimates obtained by this re-tracker mean that no meaningful statistics could be computed for the results obtained using it. Likewise, the 20Hz OCOG re-tracker is not able to detect the narrow manmade canal reliably in the period with available micro-gauge data, and thus only a single micro-gauge height value is present in the overlapping measurement period. With only a single available validation data point, no statistical computations could be made for the results obtained using this re-tracker either.
The posting rate validation test indicates that a posting rate of 700Hz gives the overall best results in terms of RMSe and Correlation, but the smaller sample size for the time series with a posting rate less than 1000Hz is likely to skew the results in their favour. The increased amount of data points offered by the 1100Hz posting rate is likely the more practical candidate due to the better data coverage that it offers.

The posting rate validation test indicates that a posting rate of 700Hz gives the overall best results in terms of RMSe and Correlation, but the smaller sample size for the time series with a posting rate less than 1000Hz is likely to skew the results in their favour. The increased amount of data points offered by the 1100Hz posting rate is likely the more practical candidate due to the better data coverage that it offers.

Based on these observations, it becomes evident that the MWaPP re-tracker is the superior choice of re-tracker for this specific area of study since it is capable of detecting the narrow manmade canal and following the trend in the dynamic height signal to a high degree.

5.2 Rhone: Port-Saint-Louis

This section presents the validation results for track S3B-199 illustrated in Figure 15. The track intersects the Rhône River at Port-Saint-Louis-du-Rhône at three locations, one of them being the inlet to an industrial access canal. Later in the analysis, we refer to the intersection of the southern part of the river and the small canal as the "Southern Crossing", and the intersection of the northern part of the river as the "Northern Crossing".

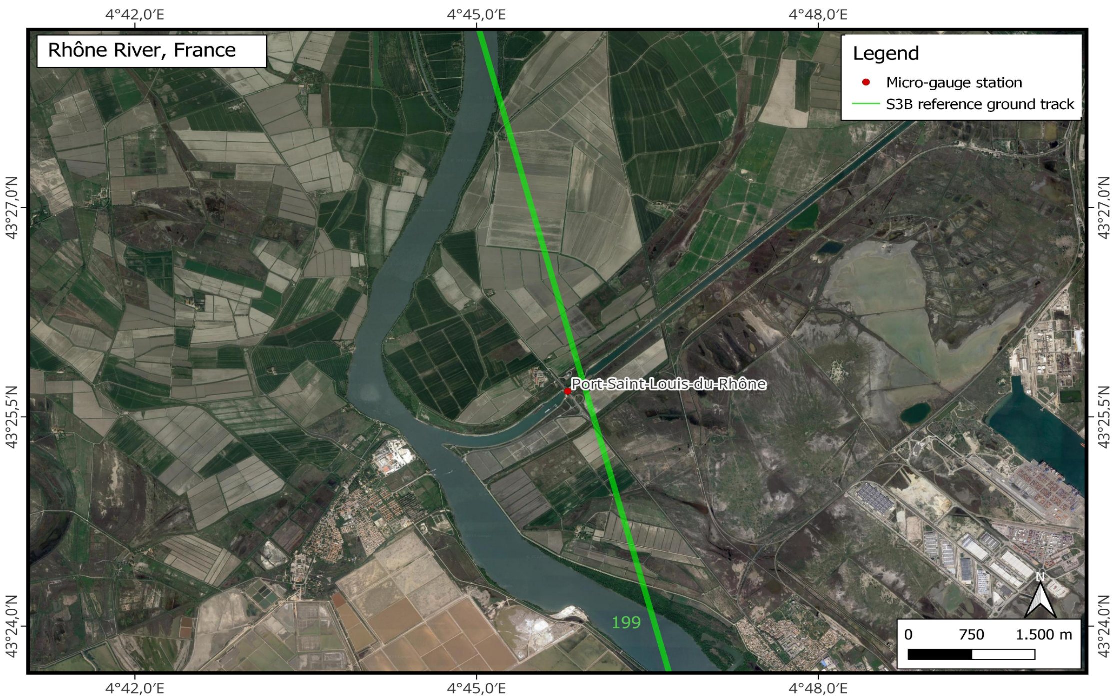

Figure 15: A map showing the location of reference ground track S3B-199 close to the mouth of the Rhône River at Port-Saint-Louis-du-Rhône. The location of the micro-gauge station installed at the beginning of an industrial access water channel by vorteX-io is also shown as a red dot. [Imagery © 2023 CNES / Airbus, Landsat / Copernicus, Maxar Technologies, Map data © 2023 Google]

5.2.1 Posting rate validation

A posting rate test was also performed for reference ground track S3B-199, using the same Hz span and re-tracker as for the test performed for reference ground track S3B-179. Time restrictions limited the scope of the validation Hz tests to only be performed using a 2.3s illumination time. The northern and southern crossings of the Rhône River were sampled separately and several time series were created for each of these ROIs within the scene. The summary statistics of the resulting validation tests can be seen in Table 7 and Table 8, and the two sets of time series can be seen illustrated in Figure 16 and Figure 17 on the following pages. The results obtained using the different posting rates are remarkably similar within each sampling region, likely due to the larger dimensions of the sampled water body making detection possible even when using posting rates below 1000Hz.

Northern Crossing

Posting rate [Hz]	Median bias [m]	RMSE [m]	RMSE Cor [m]	Correlation	#pair
500 Hz	0.461	0.481	0.148	0.523	10
600 Hz	0.462	0.482	0.151	0.497	10
700 Hz	0.466	0.489	0.158	0.479	10
800 Hz	0.463	0.488	0.159	0.454	10
900 Hz	0.464	0.483	0.153	0.493	10
1000 Hz	0.463	0.481	0.147	0.510	10
1100 Hz	0.473	0.483	0.144	0.529	10
1200 Hz	0.464	0.487	0.151	0.495	10
1300 Hz	0.463	0.484	0.148	0.520	10
1400 Hz	0.468	0.480	0.144	0.519	10
1500 Hz	0.462	0.475	0.144	0.510	10

Table 7: Summary statistics of the 2.3s illumination time Hz validation test from the northern crossing of the Rhône River.

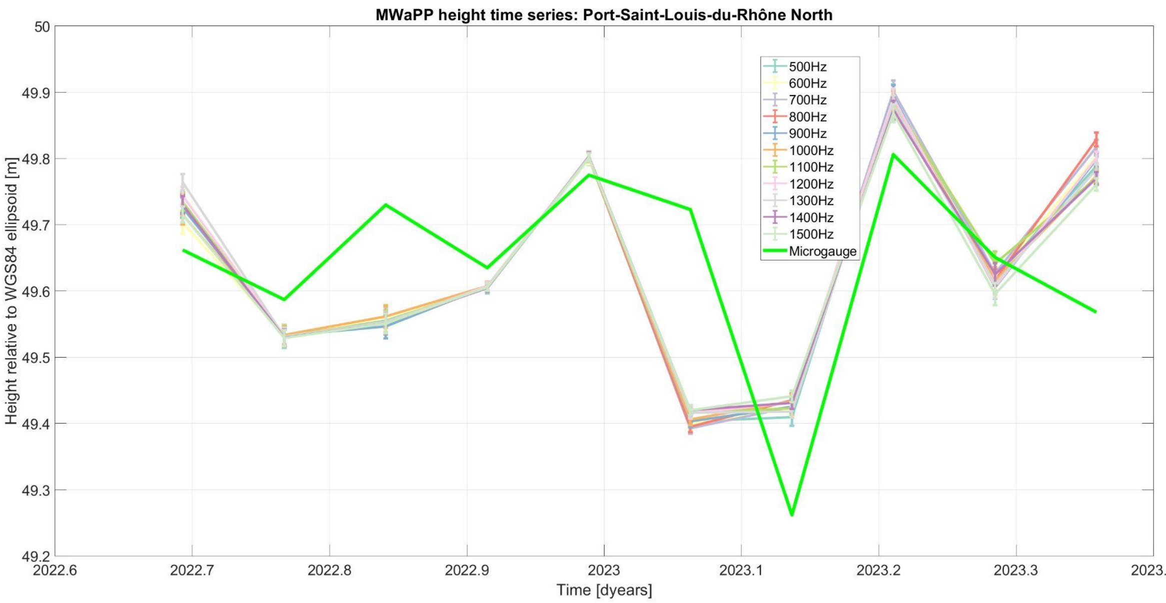

Figure 16: Time series sampled from height estimates obtained using different posting rates between 500Hz and 1500Hz and a 2.3s illumination time in the northern crossing of the Rhône River. The plotted micro-gauge estimates have been re-aligned to coincide with the time series as a group, by adding the median value of all values in the "Median Bias" column in Table 7.

Southern Crossing

Posting rate [Hz]	Median bias [m]	RMSE [m]	RMSE Cor [m]	Correlation	#pair
500 Hz	0.220	0.275	0.136	0.439	11
600 Hz	0.211	0.284	0.138	0.436	11
700 Hz	0.231	0.286	0.142	0.385	11
800 Hz	0.215	0.269	0.132	0.408	11
900 Hz	0.244	0.288	0.136	0.416	11
1000 Hz	0.214	0.275	0.130	0.428	11
1100 Hz	0.225	0.274	0.128	0.457	11
1200 Hz	0.204	0.271	0.129	0.446	11
1300 Hz	0.251	0.282	0.131	0.440	11
1400 Hz	0.227	0.283	0.131	0.434	11
1500 Hz	0.230	0.281	0.130	0.445	11

Table 8: Summary statistics of the 2.3s illumination time Hz validation test from the northern crossing of the Rhône River.

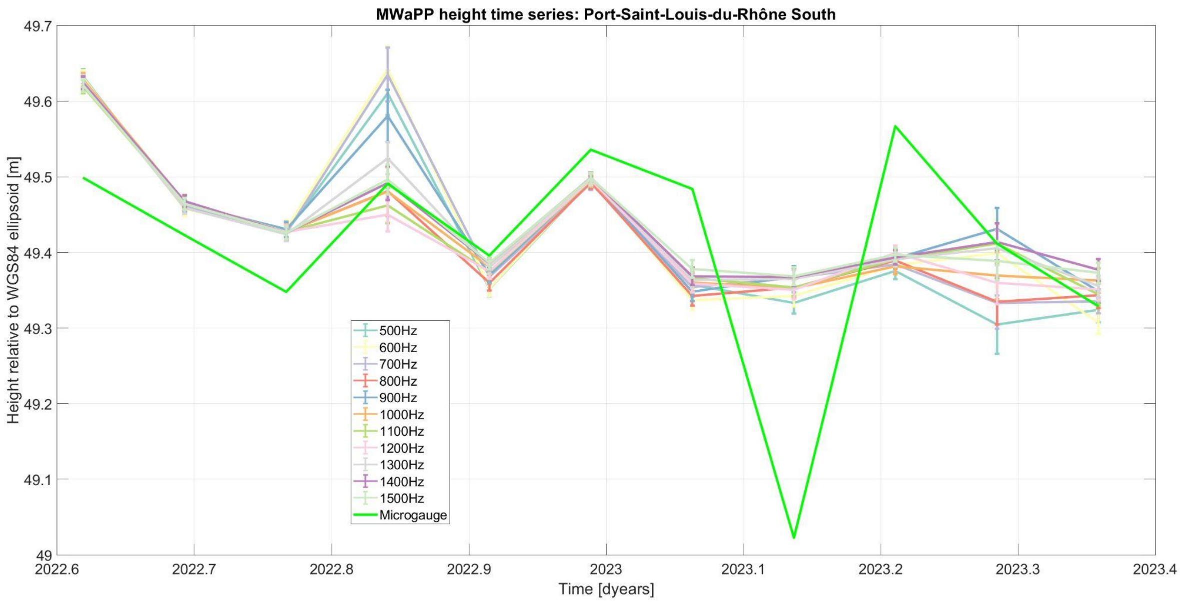

Figure 17: Time series sampled from height estimates obtained using different posting rates between 500Hz and 1500Hz and a 2.3s illumination time in the southern crossing of the Rhône River. The plotted micro-gauge estimates have been re-aligned to coincide with the time series as a group, by adding the median value of all values in the "Median Bias" column in Table 8.

5.2.2 FFSAR re-tracker validation

In this section, the FFSAR water levels derived from different re-trackers with a posting rate of 1000 Hz are evaluated for the Port-Saint-Louis-du-Rhône area.

Figure 18,20,22a and 24 shows the FFSAR water levels as a function of latitude processed with the PTR, Multi-PTR, OCOG, and MWaPP re-trackers, respectively. The blue data points indicate measurements that originate from the "open" Rhône River, the red data points indicate measurements that originate from within the industrial access canal leading into the harbour area, the black data points represent ICESat-2 measurements from the area, and the green data point with error bar represents the water level range of the gauge station. The micro-gauge station in this scene is mounted on an access gate that may be opened or close, changing the water height in the access channel as a result. The water height in the southern crossing of the river and the access channel are both comparable with the water level observed by the micro-gauge.

Figures 19, 21, 23, and 25 display the estimated water level time series for the two water bodies, the southern crossing (red) and the northern crossing (blue). The water level as observed by the micro-gauge stations has been plotted as a time series along with these (green) and has been re-aligned with the re-tracker estimates by adding the median bias between the respective time series data and micro-gauge data points. The equivalent time series based on the standard 20 Hz (OCOG) is shown in Figure 26. The summary statistics, RMSE, and Correlation are reported in Tables 9 and 10.

PTR re-tracker

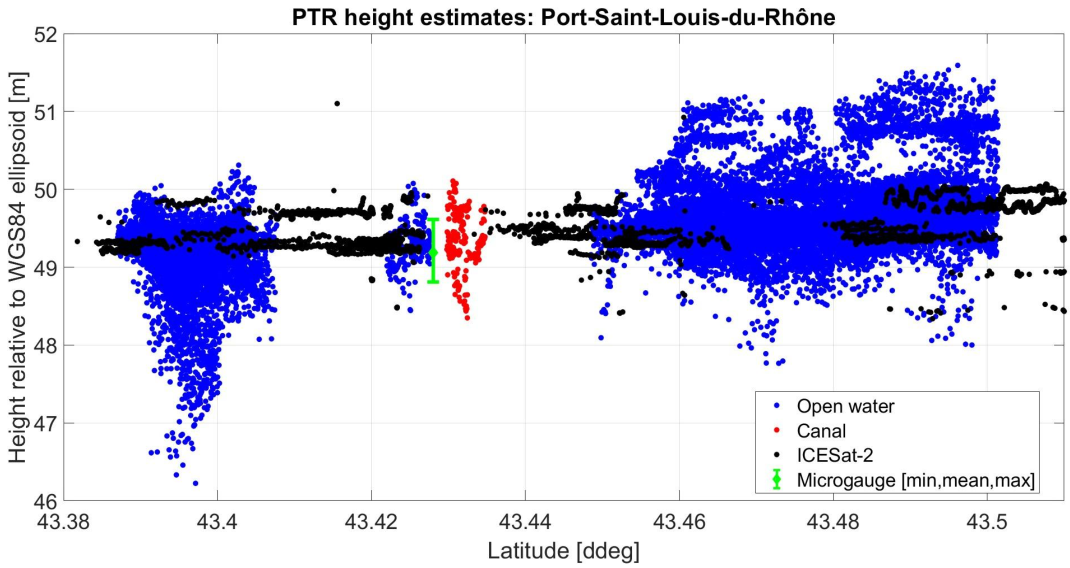

Figure 18: FFSAR water levels estimated by the PTR re-tracker as a function of latitude. The blue and red lines show the dynamic signal of the water levels in the northern and southern crossings of the Rhône River respectively. The black data points are ICESat-2 data with the same spatial and temporal origin as the input data processed by the re-tracker. The green error bar represents the variance in the observed micro-gauge signal, with the minimum, median and maximum values defining a reference interval.

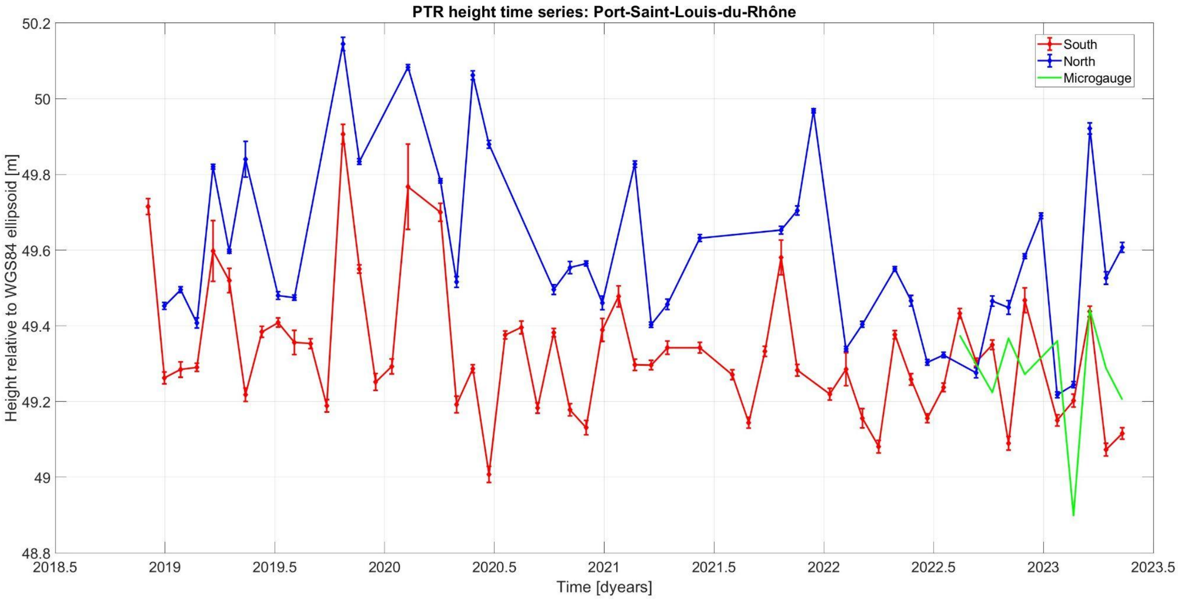

Figure 19: Time series of FFSAR water levels estimated by the PTR re-tracker. The blue and red lines show the dynamic signal of the water levels in the northern and southern crossings of the Rhône River respectively. The green line shows the dynamic signal of the water level at the start of an industrial access canal where the micro-gauge station is placed in the ROI.

MultiPTR re-tracker

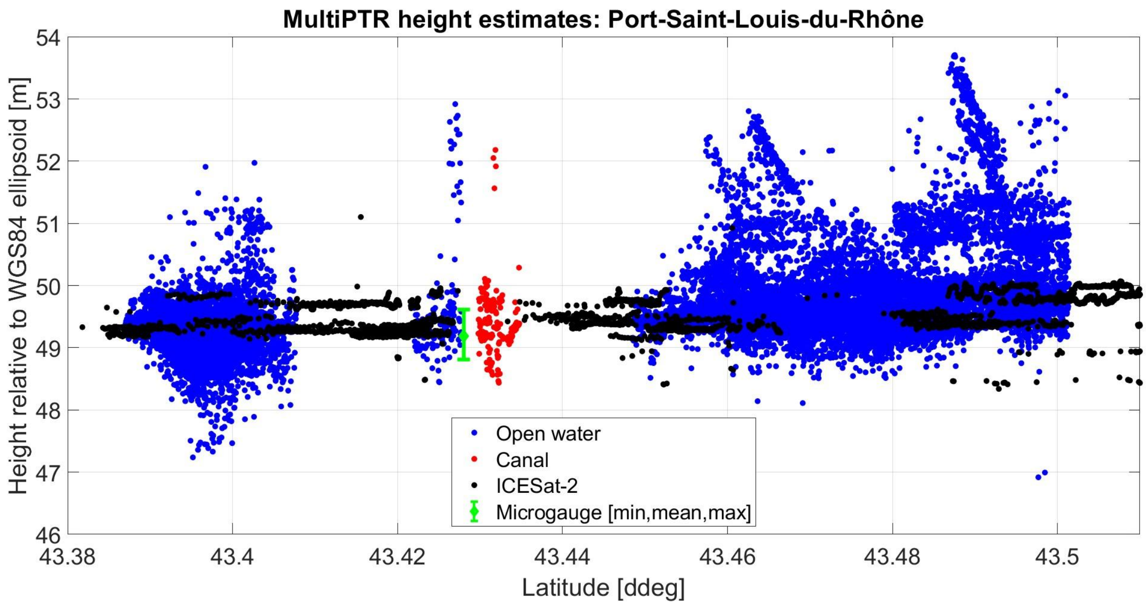

Figure 20: FFSAR water levels estimated by the MultiPTR re-tracker as a function of latitude. The water levels are temporally dispersed throughout the period of analysis highlighted in Table 2 RON 199. The blue and red lines show the dynamic signal of the water levels in the northern and southern crossings of the Rhône River respectively. The black data points are ICESat-2 data with the same spatial and temporal origin as the input data processed by the re-tracker. The green error bar represents the variance in the observed micro-gauge signal, with the minimum, median and maximum values defining a reference interval.

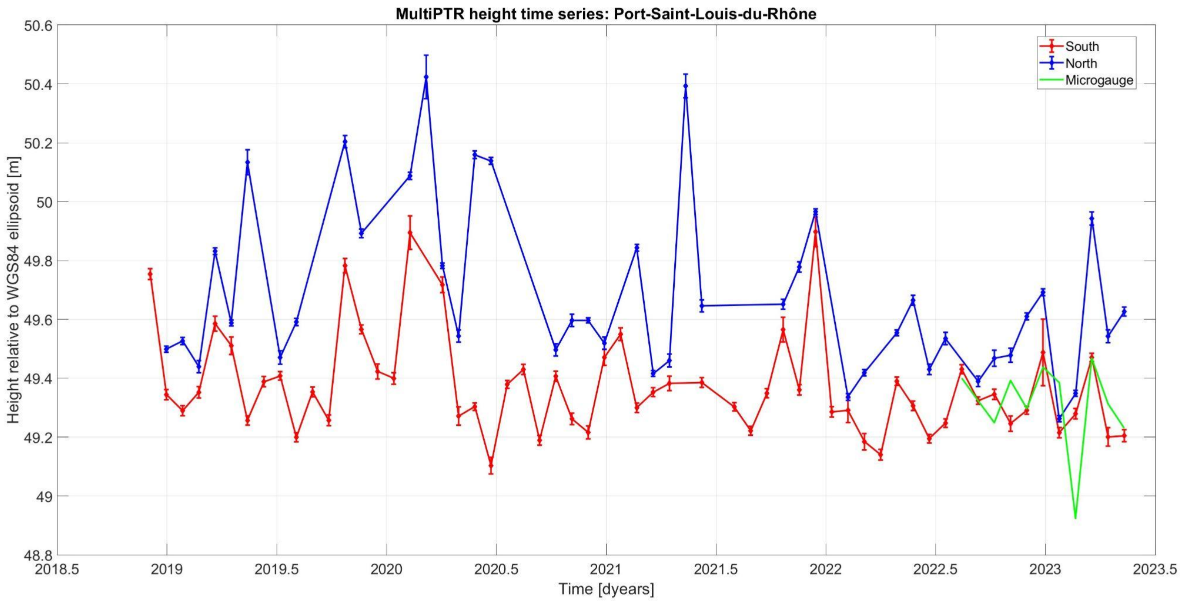

Figure 21: Time series of FFSAR water levels estimated by the MultiPTR re-tracker. The blue and red lines show the dynamic signal of the water levels in the northern and southern crossings of the Rhône River respectively. The green line shows the dynamic signal of the water level at the start of an industrial access canal where the micro-gauge station is placed in the ROI.

OCOG re-tracker

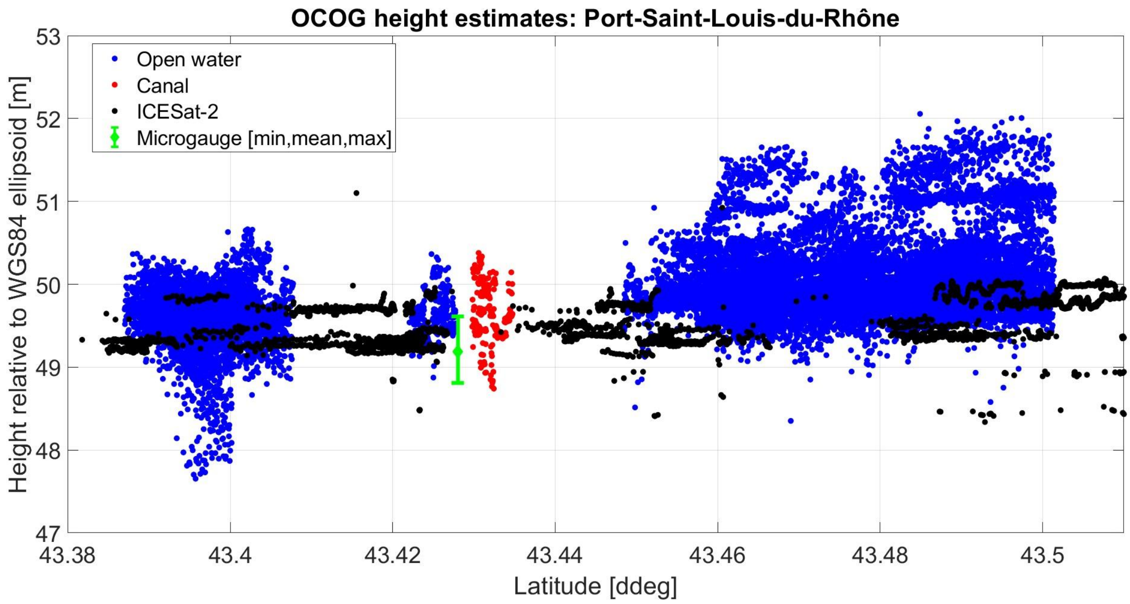

Figure 22: FFSAR water levels estimated by the OCOG re-tracker as a function of latitude. The blue and red lines show the dynamic signal of the water levels in the northern and southern crossings of the Rhône River respectively. The black data points are ICESat-2 data with the same spatial and temporal origin as the input data processed by the re-tracker. The green error bar represents the variance in the observed micro-gauge signal, with the minimum, median and maximum values defining a reference interval.

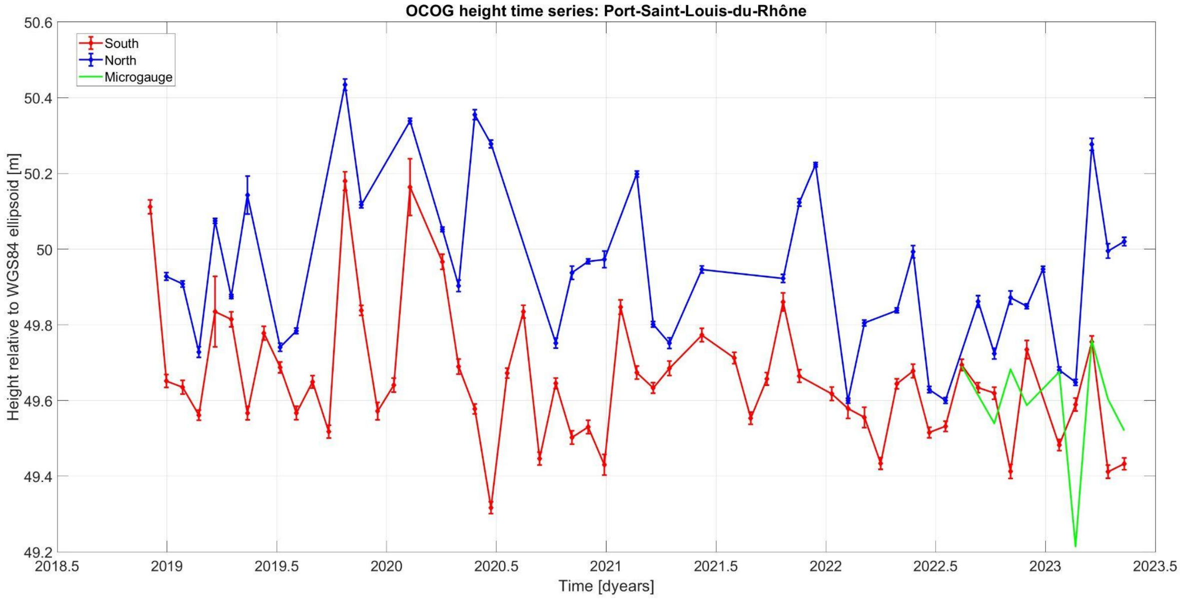

Figure 23: Time series of FFSAR water levels estimated by the OCOG re-tracker. The blue and red lines show the dynamic signal of the water levels in the northern and southern crossings of the Rhône River respectively. The green line shows the dynamic signal of the water level at the start of an industrial access canal where the micro-gauge station is placed in the ROI.

MWaPP re-tracker

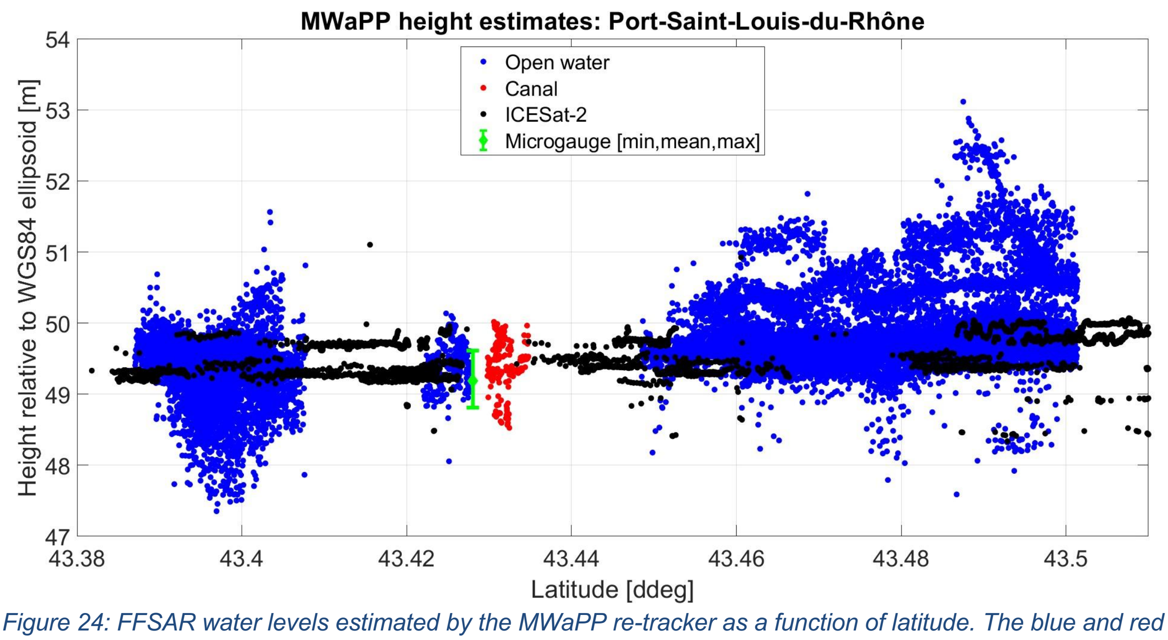

Figure 24: FFSAR water levels estimated by the MWaPP re-tracker as a function of latitude. The blue and red lines show the dynamic signal of the water levels in the northern and southern crossings of the Rhône River respectively. The black data points are ICESat-2 data with the same spatial and temporal origin as the input data processed by the re-tracker. The green error bar represents the variance in the observed micro-gauge signal, with the minimum, median and maximum values defining a reference interval.

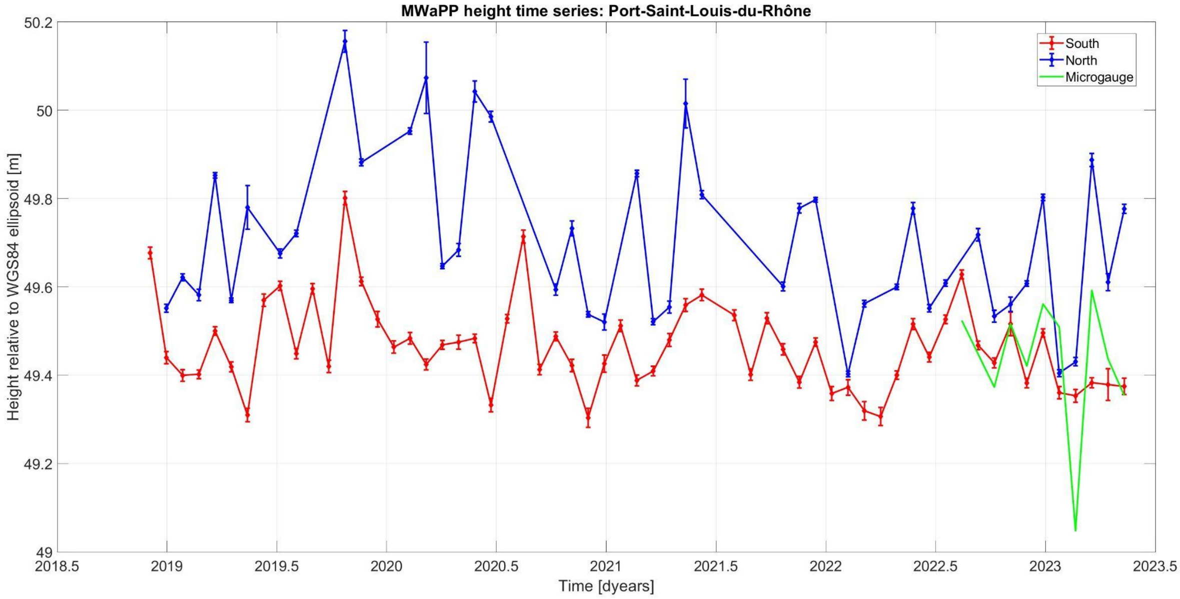

Figure 25: Time series of FFSAR water levels estimated by the MWaPP re-tracker. The blue and red lines show the dynamic signal of the water levels in the northern and southern crossings of the Rhône River respectively. The green line shows the dynamic signal of the water level at the start of an industrial access canal where the micro-gauge station is placed in the ROI.

ESA 20Hz OCOG re-tracker

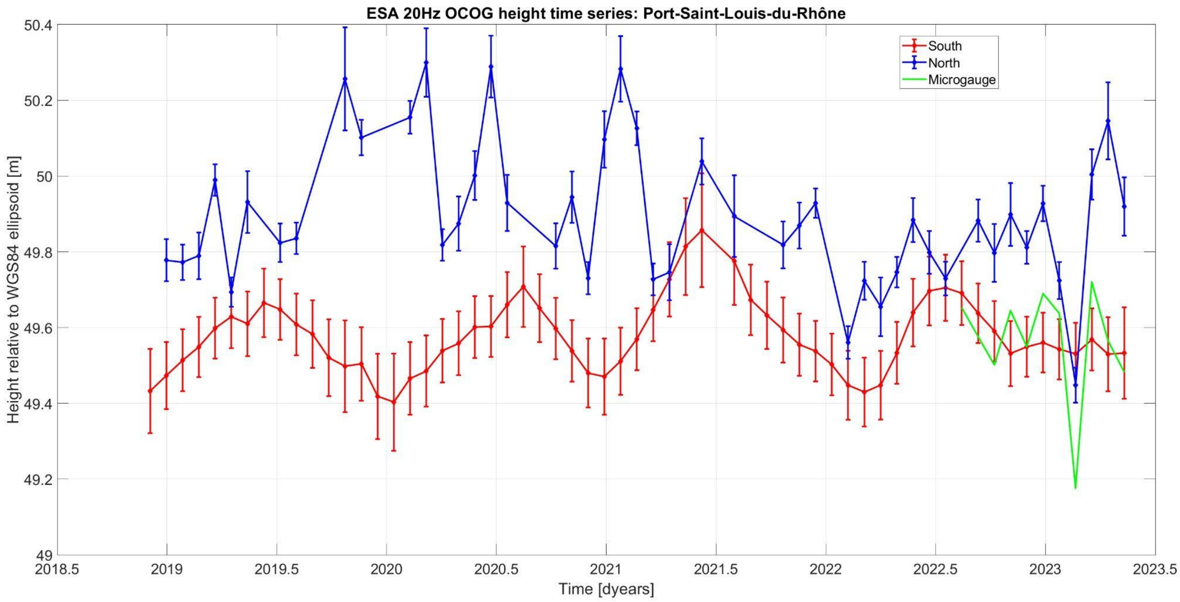

Figure 26: Time series of water levels estimated by the standard 20Hz OCOG re-tracker. The blue and red lines show the dynamic signal of the water levels in the northern and southern crossings of the Rhône River respectively. The green line shows the dynamic signal of the water level at the start of an industrial access canal where the micro-gauge station is placed in the ROI.

5.2.3 Summary of findings for Port-Saint-Louis-du-Rhône

The resulting height estimates from the employed re-trackers all follow the trend in the change of water level observed by the micro-gauge to varying degrees. A set of summary statistics for the various re-trackers can be seen in Table 9 and Table 10.

Northern Crossing

Retracker	Median bias [m]	RMSE [m]	RMSE Cor [m]	Correlation	#pair
PTR	0.36	0.37	0.21	0.47	10
MultiPTR	0.38	0.39	0.21	0.40	10
OCOG	0.66	0.73	0.17	0.55	10
MWaPP	0.46	0.46	0.15	0.63	10
20Hz OCOG	0.67	0.77	0.23	0.49	10

Table 9: Summary statistics for the different re-trackers in the northern crossing of the Rhône River.

Southern Crossing

Retracker	Median bias [m]	RMSE [m]	RMSE Cor [m]	Correlation	#pair
PTR	0.07	0.22	0.22	0.23	10
MultiPTR	0.12	0.18	0.20	0.41	11
OCOG	0.41	0.44	0.18	0.10	10
MWaPP	0.18	0.22	0.20	0.35	11
20Hz OCOG	0.38	0.41	0.14	0.29	11

Table 10: Summary statistics for the different re-trackers in the southern crossing of the Rhône River.

From both Table 9 and Table 10, it is immediately apparent that the correlation between the estimates obtained from the different re-trackers and the micro-gauge values is low across the board. This can be explained by the fact that the height range in most of the time series is approximately 1m. The small range in observed height values means that even small deviations from the trend observed by the micro-gauge will lead to a significant loss in correlation.

The RMSE values obtained from the PTR, MultiPTR, and MWaPP re-trackers in both the northern and southern crossings are noticeably better than the values obtained from the OCOG and 20Hz OCOG re-trackers in their respective crossing. While all three re-trackers have similar RMSE values in the southern crossing, the RMSE value obtained for the MWaPP re-tracker is however slightly worse in the northern crossing when compared to the RMSE values from the PTR and MultiPTR re-trackers. Overall, it seems however that the PT, MultiPTR, and MWaPP re-trackers are all capable of accurately measuring the water surface height in the Rhône River near Port-Saint-Louis-du-Rhône. The only noticeable deviation between their estimates and the reference micro-gauge values is a noticeable drop in water height in the industrial access channel occurring somewhere in early 2023. All the re-tracker time series deviates from the trend observed by the micro-gauge by a maximum of approximately 20cm.

Comparing the time series in Figures 19, 21, 23, 25, and 26 reveals that the time series for the MWaPP re-tracker sampled at the southern crossing follows the trend observed by the micro-gauge quite well at the beginning of the overlapping sensing period. It does however deviate later where a noticeable drop in water height occurs within the industrial access channel, which none of the employed re-trackers are capable of detecting in the southern crossing.

The posting rate validation test all results in very similar statistical results within each crossing. This means that the scene is almost equally well observed by the SMAP using the different posting rates. The scene is relatively simple and homogenous, and the river is relatively large com to the Fos-Sur-Mer canal. A high posting rate, with an associated increase in processing time, is therefore unlikely to offer any benefit for this type of scene.

These factors combined means that the PTR, MultiPTR, and MWaPP re-trackers all provide the comparatively best results for the Port-Saint-Louis-du-Rhône scene, while none of the three re-trackers stand out as the superior option among them.

5.3 Severn Estuary

This section presents the validation results for track S3B-265 illustrated in Figure 27. The track crosses the southern bank of the Severn Estuary close to Hinkley Port in the UK, passing by the micro-gauge station placed in Weston-super-Mare, and crosses the northern bank close to the mouth of River Usk in the town of Newport (Wales) where a second micro-gauge station is placed on a bridge over the river.

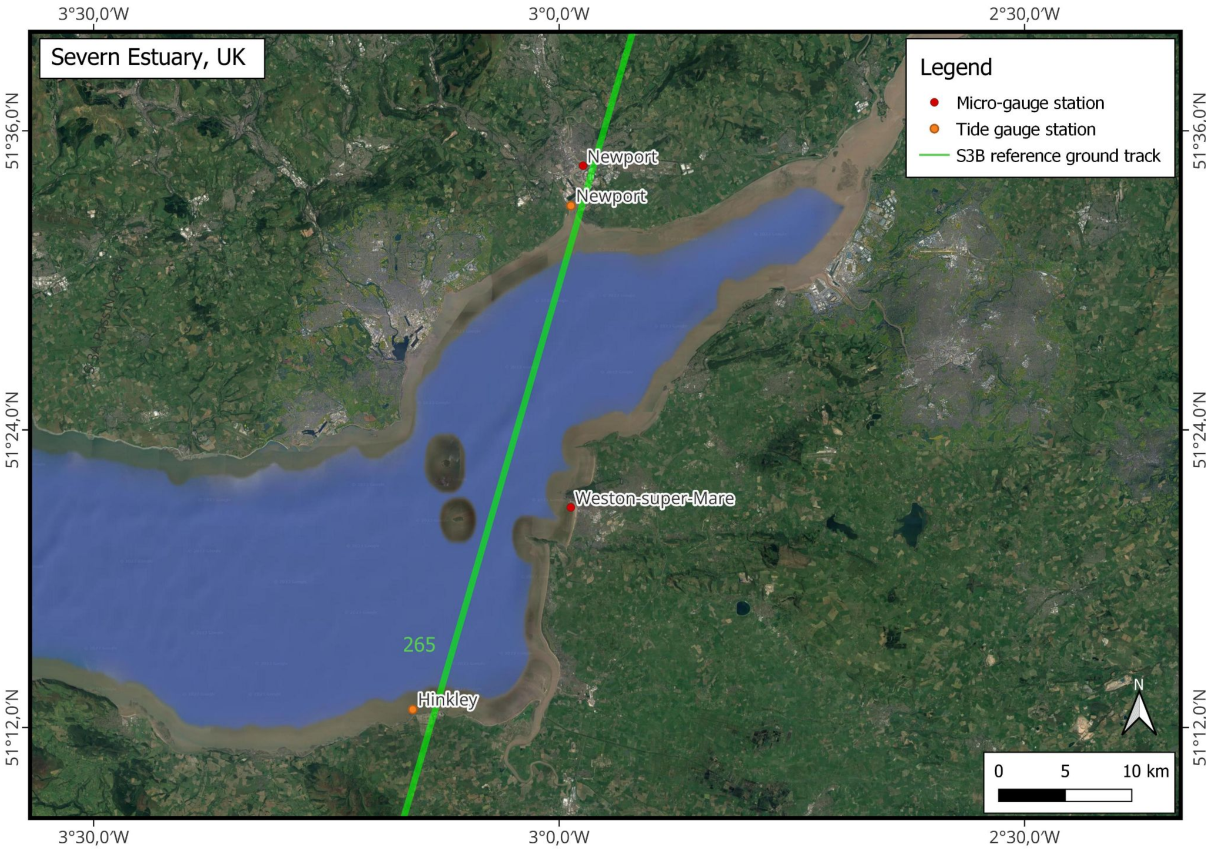

Figure 27: A map showing the location of the ground track for RON 265 in the Severn Estuary lying at the end of the Bristol Channel, UK. The location of the vorteX-io micro-gauge stations and NOC tide gauge stations are marked as red and orange dots respectively. [Imagery © 2023 TerraMetrics, Map data © 2023 Google]

5.3.1 FFSAR re-tracker validation

In this section, the FFSAR water levels derived from different re-trackers with a posting rate of 1000 Hz are evaluated for the Severn Estuary.

Figures 28, 30, 32, and 34 show the FFSAR water levels as a function of latitude processed with the PTR, Multi-PTR, OCOG, and MWaPP re-trackers, respectively. The blue data points indicate measurements that originate from the open water areas in the Severn Estuary, the red data points indicate measurements that originate from the mouth of River Usk, the black data points represent ICESat-2 measurements from the area, and the green and magenta data points with error bar represents the water level range of the gauge stations mounted in the study area at Newport and Weston-super-Mare respectively.

Figures 29, 31, 33, and 35 display the estimated water level time series for the two water bodies: the mouth of River Usk (red) and the open water areas in Severn Estuary (blue). The water level as observed by the micro-gauge stations has been plotted as a time series along with these (green/magenta) and has been re-aligned with the re-tracker estimates by adding the median bias between the respective time series data and micro-gauge data points. The equivalent time series based on the standard 20 Hz (OCOG) is shown in Figure 38.

Figures 36 and 37 depict the water level time series estimated by the MWaPP re-tracker plotted alongside the water level heights observed by the pre-existing National Tide and Sea level Facility (NTSLF) tide gauges at Newport and Hinkley. The water level time series for the mouth of River Usk (red) and the open water areas in Severn Estuary (blue) are plotted in the same fashion as seen in Figure 35, along with the trend observed by the Newport (green) and Hinkley (magenta) tide gauges. The tide gauge water heights have been realigned in the same manner as the micro-gauges, by adding the median bias between the respective time series data and tide gauge data points.

The summary statistics, RMSE, and Correlation are reported in Tables 11 and 12 for the validation performed with the micro-gauge measurements. Table 13 present the validation performed for the MWaPP re-tracker performed with the NTSLF Newport and Hinkley tide gauges in the Severn.

PTR re-tracker

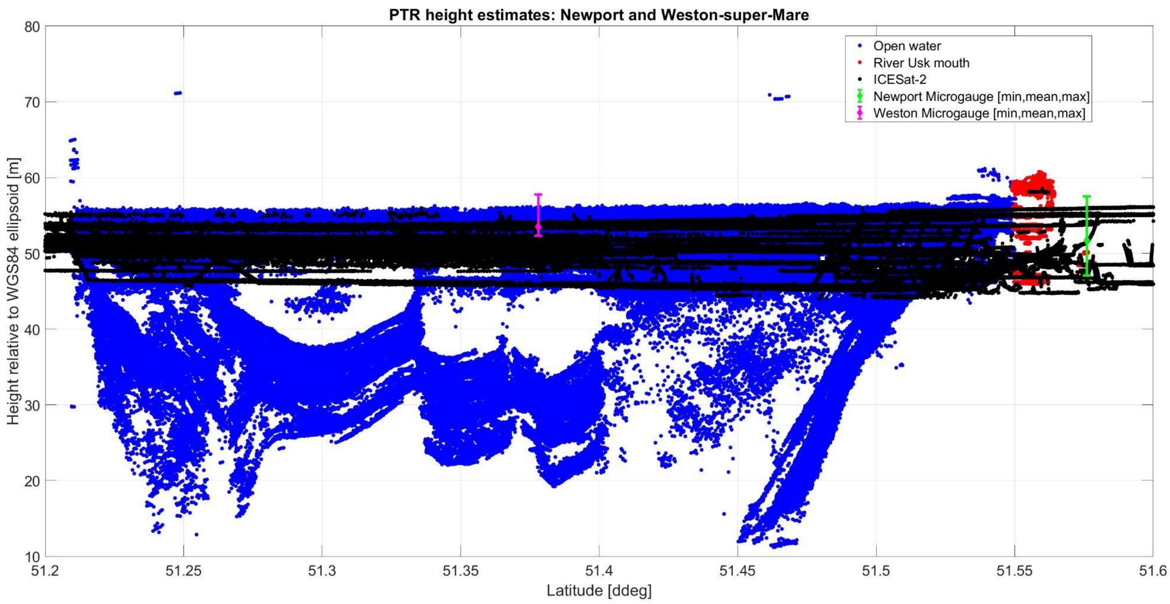

Figure 28: FFSAR water levels estimated by the PTR re-tracker as a function of latitude. The water levels are temporally dispersed throughout the period of analysis highlighted in Table 1 RON 265. The blue and red data points originate from the open water area in the Severn Estuary and the mouth of River Usk respectively. The black data points are ICESat-2 data with the same spatial and temporal origin as the input data processed by the re-tracker. The green and magenta error bars represent the variance in the observed micro-gauge signals at Newport and Weston-super-Mare respectively, with the minimum, median and maximum values defining a reference interval.

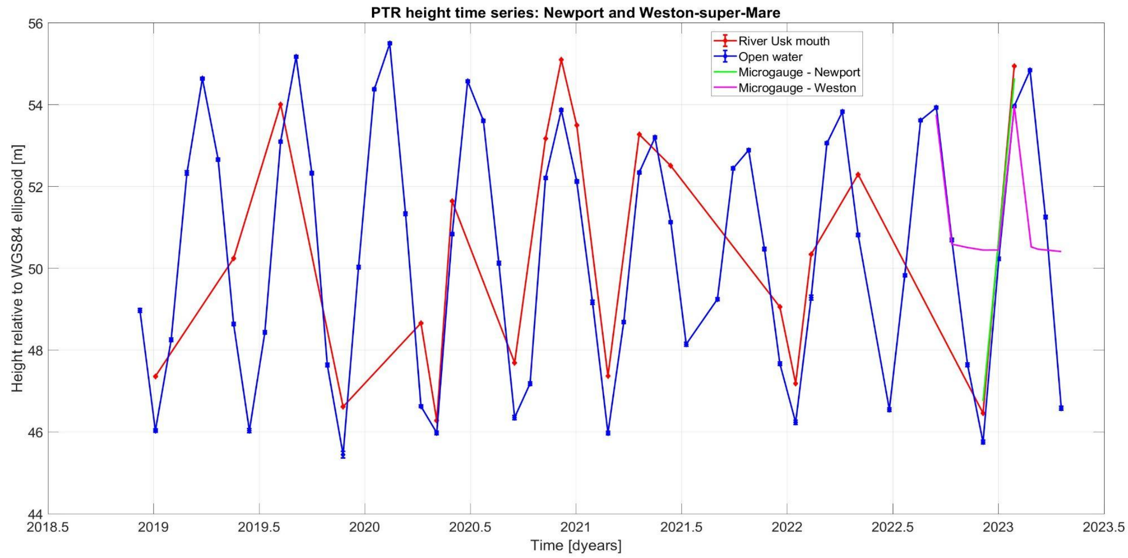

Figure 29: Time series of FFSAR water levels estimated by the PTR re-tracker. The blue and red data points originate from the open water area of the Severn Estuary and the mouth of River Usk respectively. The green and magenta lines show the dynamic signals of the water levels measured at Newport and Weston-super-Mare micro-gauge stations respectively.

MultiPTR re-tracker

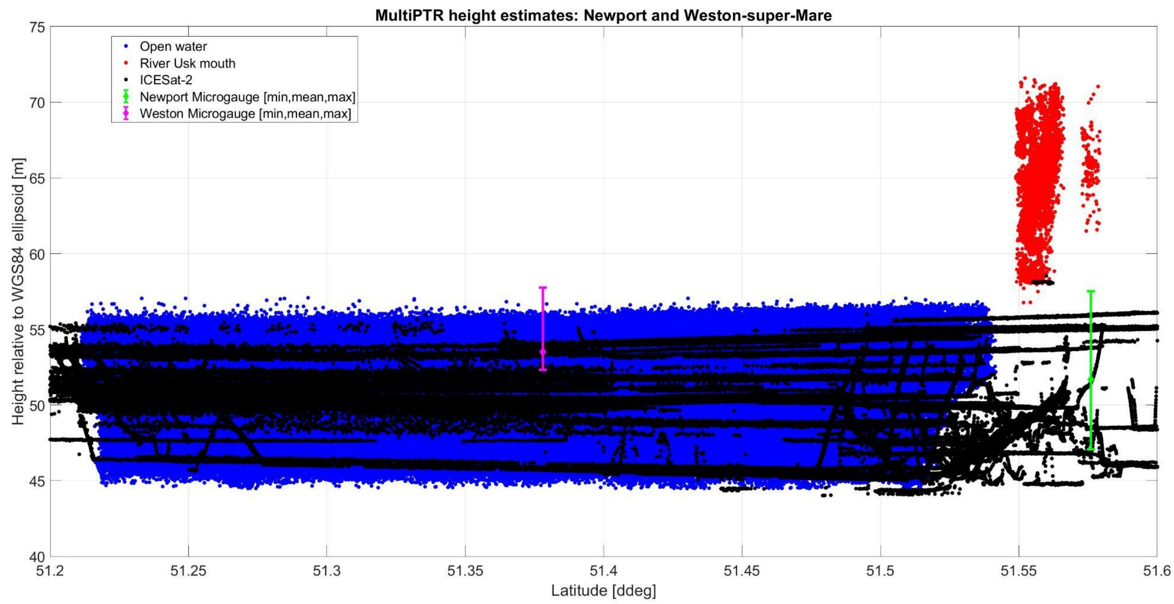

Figure 30: FFSAR water levels estimated by the MultiPTR re-tracker as a function of latitude. The water levels are temporally dispersed throughout the period of analysis highlighted in Table 1 RON 265. The blue and red data points originate from the open water area in the Severn Estuary and the mouth of River Usk respectively. The black data points are ICESat-2 data with the same spatial and temporal origin as the input data processed by the re-tracker. The green and magenta error bars represent the variance in the observed micro-gauge signals at Newport and Weston-super-Mare respectively, with the minimum, median and maximum values defining a reference interval.

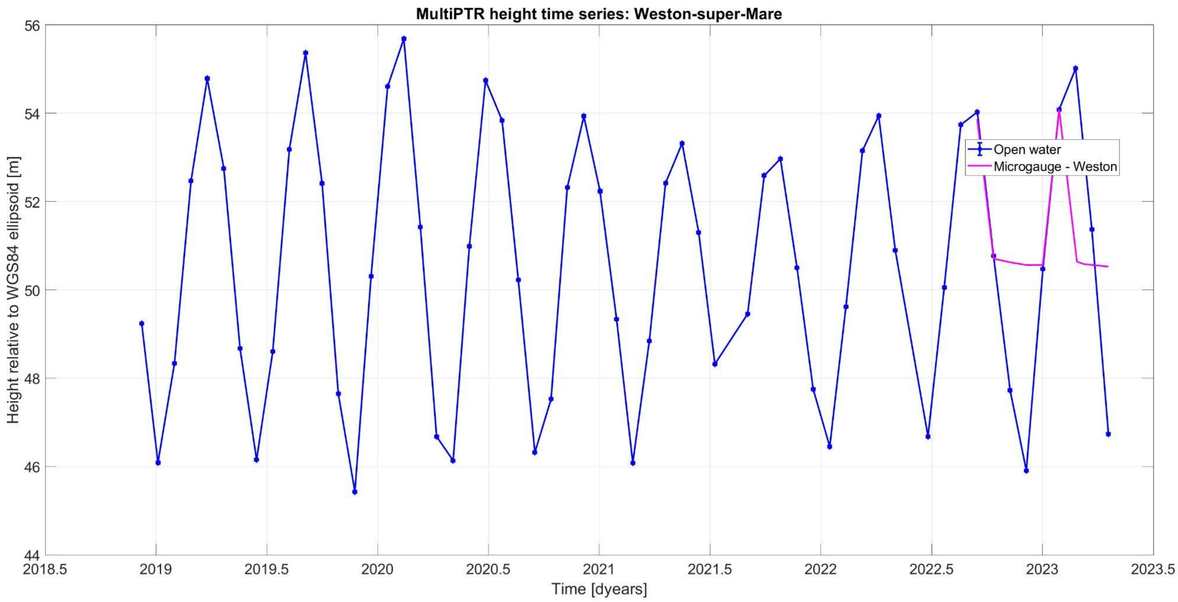

Figure 31: Time series of FFSAR water levels estimated by the MultiPTR re-tracker. The blue and red data points originate from the open water area of the Severn Estuary and the mouth of River Usk respectively. The green and magenta lines show the dynamic signals of the water levels measured at Newport and Weston-super-Mare micro-gauge stations respectively.

OCOG re-tracker

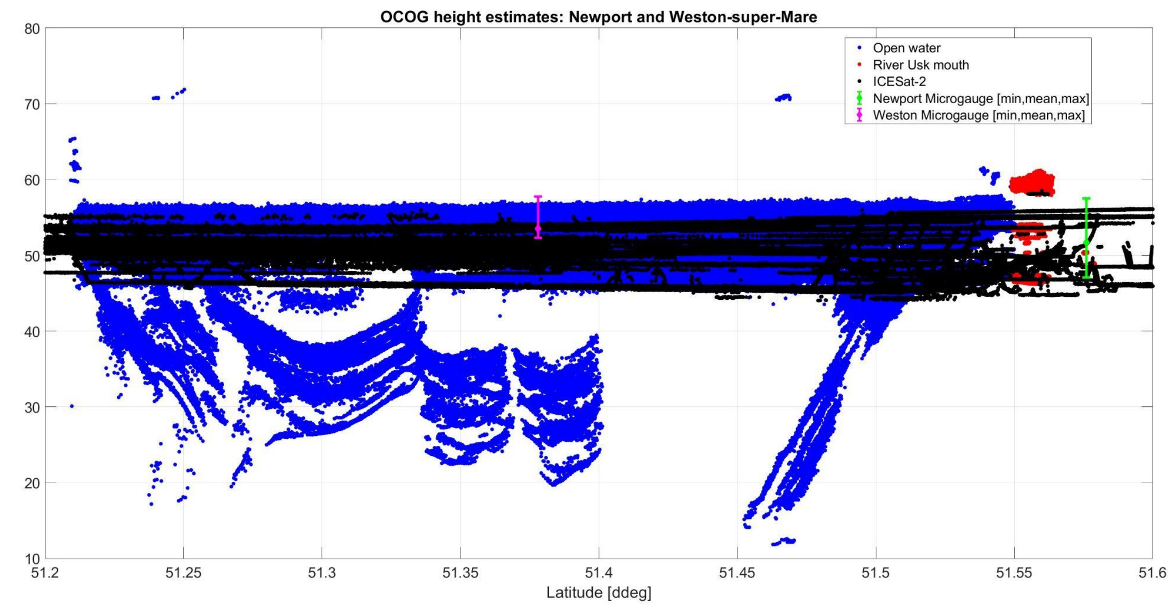

Figure 32: FFSAR water levels estimated by the OCOG re-tracker as a function of latitude. The water levels are temporally dispersed throughout the period of analysis highlighted in Table 1 RON 265. The blue and red data points originate from the open water area in the Severn Estuary and the mouth of River Usk respectively. The black data points are ICESat-2 data with the same spatial and temporal origin as the input data processed by the re-tracker. The green and magenta error bars represent the variance in the observed micro-gauge signals at Newport and Weston-super-Mare respectively, with the minimum, median and maximum values defining a reference interval.

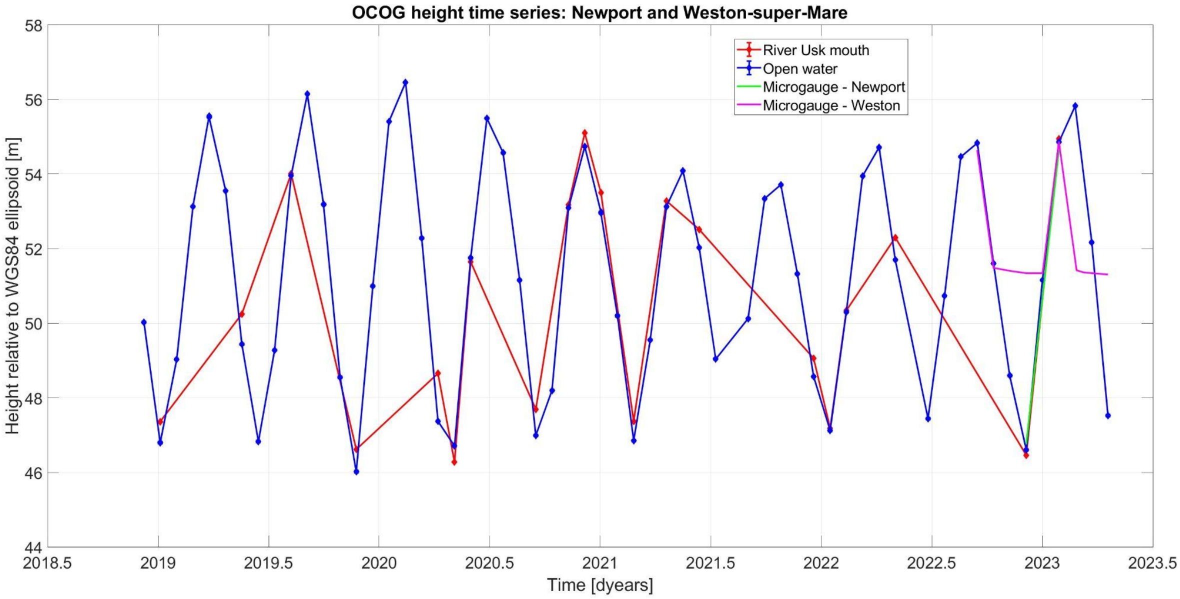

Figure 33: Time series of FFSAR water levels estimated by the OCOG re-tracker. The blue and red data points originate from the open water area of the Severn Estuary and the mouth of River Usk respectively. The green and magenta lines show the dynamic signals of the water levels measured at Newport and Weston-super-Mare micro-gauge stations respectively.

MWaPP re-tracker

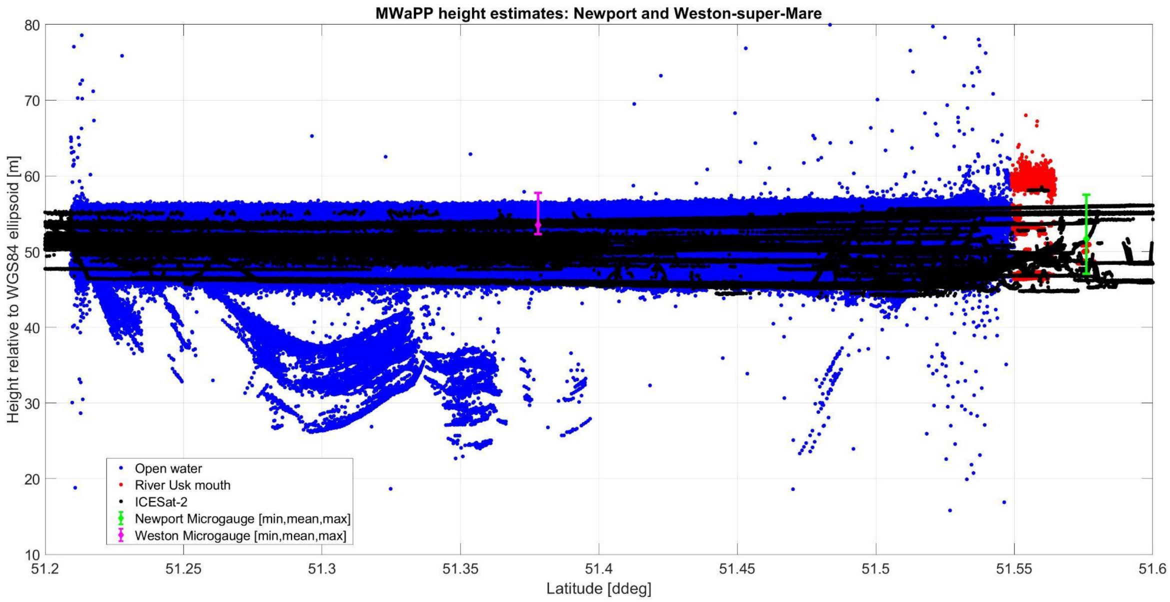

Figure 34: FFSAR water levels estimated by the MWaPP re-tracker as a function of latitude. The water levels are temporally dispersed throughout the period of analysis highlighted in Table 1 RON 265. The blue and red data points originate from the open water area in the Severn Estuary and the mouth of River Usk respectively. The black data points are ICESat-2 data with the same spatial and temporal origin as the input data processed by the re-tracker. The green and magenta error bars represent the variance in the observed micro-gauge signals at Newport and Weston-super-Mare respectively, with the minimum, median and maximum values defining a reference interval.

Micro-gauge reference (Newport and Weston Super Mare)

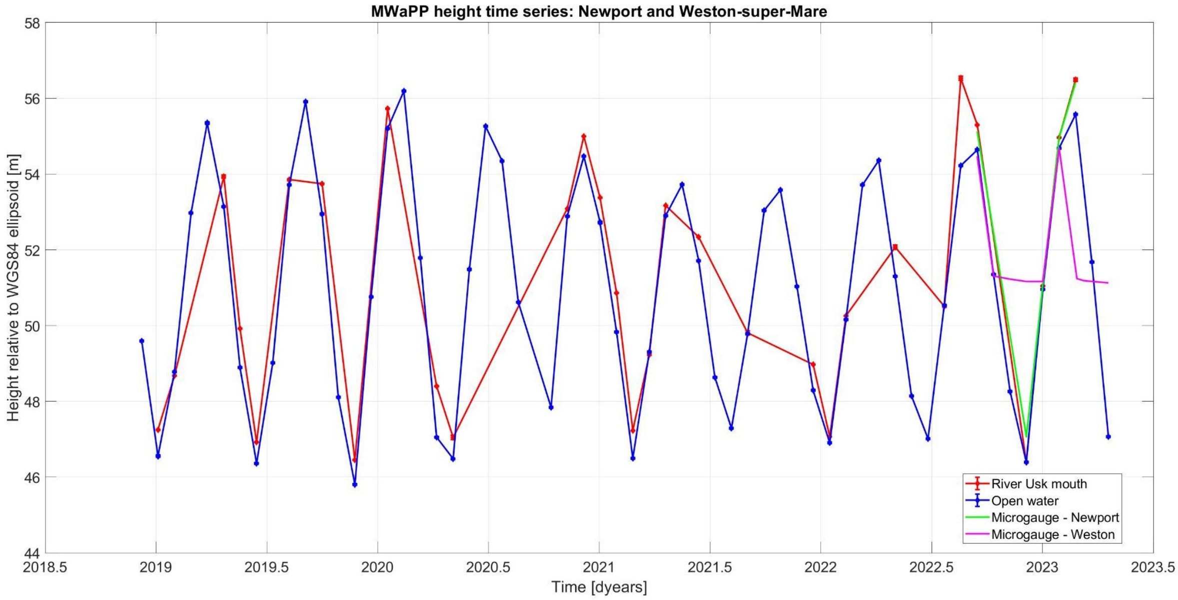

Figure 35: Time series of FFSAR water levels estimated by the MWaPP re-tracker. The blue and red data points originate from the open water area of the Severn Estuary and the mouth of River Usk respectively. The green and magenta lines show the dynamic signals of the water levels measured at Newport and Weston-super-Mare micro-gauge stations respectively.

NTSLF Tidal gauge reference (Newport and Hinkley)

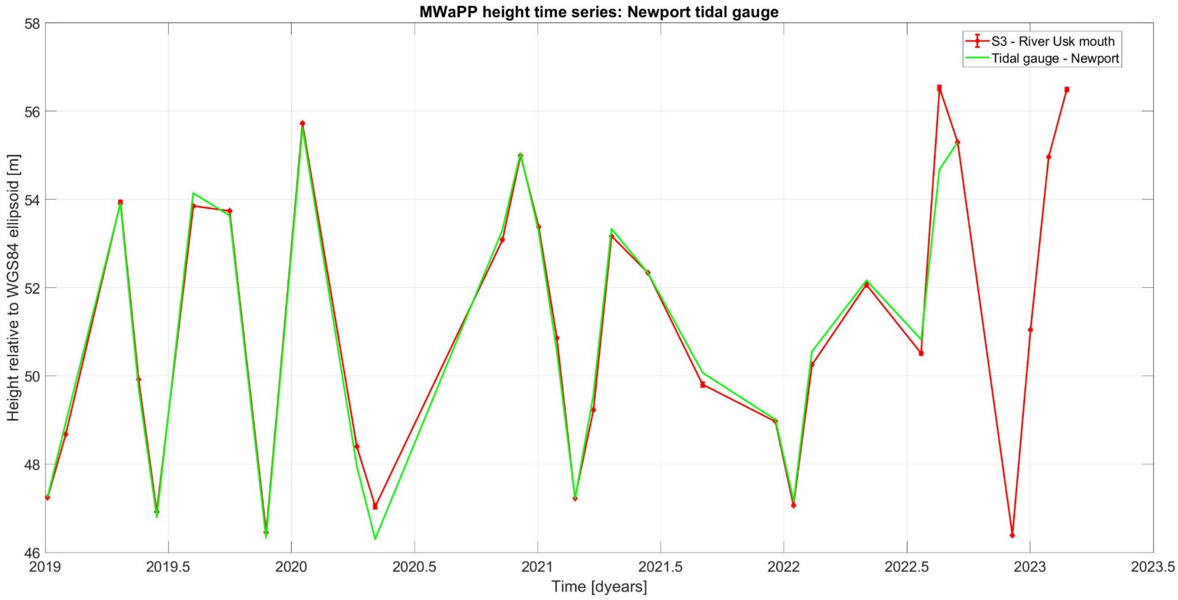

Figure 36: Time series of FFSAR water levels in the mouth of River Usk estimated by the MWaPP re-tracker from Sentinel-3 data (red) and re-aligned tidal gauge reference data measured by the Newport tide gauge (green).

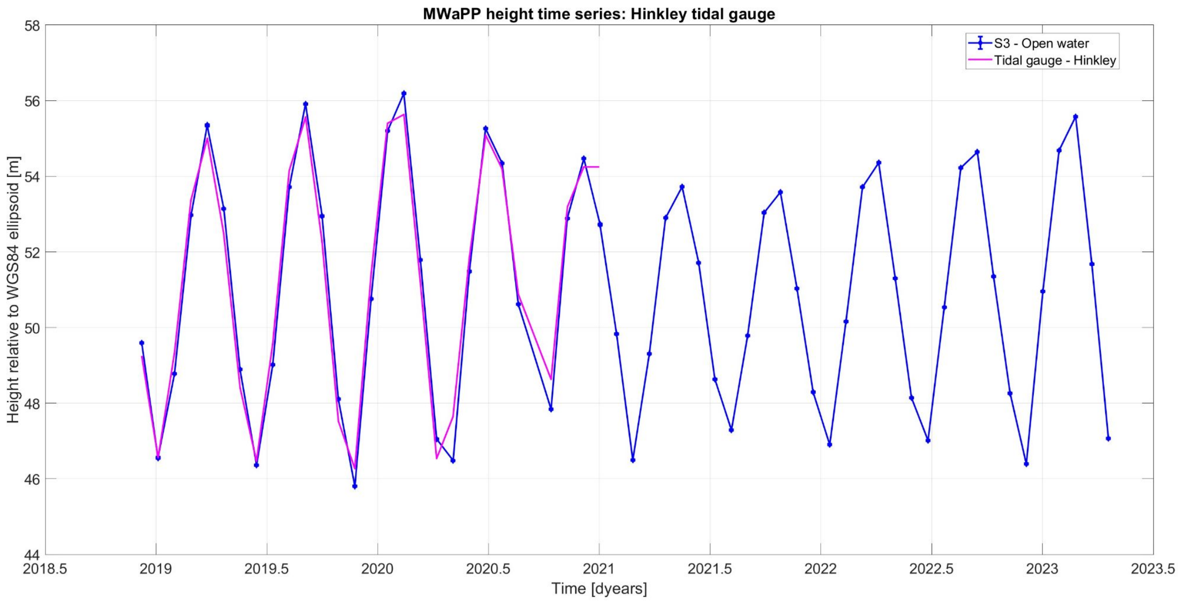

Figure 37: Time series of FFSAR water levels in the open water area of the Severn Estuary estimated by the MWaPP re-tracker from Sentinel-3 data (blue) and re-aligned tidal gauge reference data measured by the Hinkley tide gauge (magenta). Data from 2021 onwards have been removed from the tide gauge data set in order to negate it's fluence on statistical computations.

ESA 20Hz OCOG re-tracker

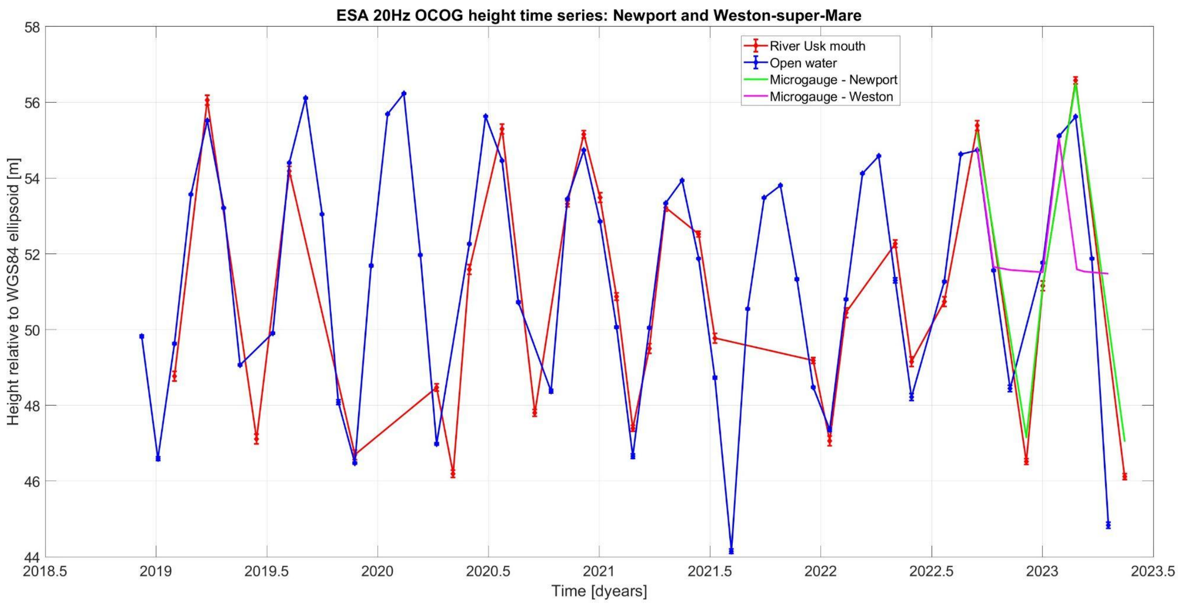

Figure 38: Time series of water levels estimated by the standard 20Hz OCOG re-tracker. The blue and red data points originate from the open water area of the Severn Estuary and the mouth of River Usk respectively. The green and magenta lines show the dynamic signals of the water levels measured at Newport and Weston-super-Mare micro-gauge stations respectively.

5.3.2 Summary of findings for the Severn Estuary

The resulting height estimates from the employed re-trackers all follow the trend in the change of water level observed by the micro-gauge to varying degrees. A set of summary statistics for the various re-trackers can be seen in Table 11 and Table 12.

Severn: Newport Micro-gauge

Retracker	Median bias [m]	RMSE [m]	RMSE Cor [m]	Correlation	#pair
PTR	-0.50	0.66	0.31	1.00	4
MultiPTR	-	-	-	-	-
OCOG	-0.54	0.61	0.29	1.00	2
MWaPP	-0.224	0.435	0.314	0.998	5
20Hz OCOG	-0.137	0.590	0.508	0.999	5

Table 11: Summary statistics for the estimates obtained with the different re-trackers in the part of the crossing close to the Newport micro-gauge station.

Severn: Weston-super-Mare Micro-gauge

Retracker	Median bias [m]	RMSE [m]	RMSE Cor [m]	Correlation	#pair
PTR	-1.40	1.40	0.54	0.99	9
MultiPTR	-1.30	1.30	0.52	0.99	9
OCOG	-0.52	0.68	0.55	0.99	9
MWaPP	-0.224	0.435	0.314	0.998	9
20Hz OCOG	-0.137	0.590	0.508	0.999	8

Table 12: Summary statistics for the estimates obtained with the different re-trackers in the part of the crossing close to the Weston-super-Mare micro-gauge station.

Severn: Newport and Hinkley NTSLF tide gauges (MWaPP)

Tide gauge	Ellipsoid Offset [m]	Median bias [m]	RMSE [m]	RMSE Cor [m]	Correlation	#pair
Newport	50.65	-5.71	5.66	0.43	0.99	27
Hinkley	50.86	-0.286	0.644	0.55	0.98	32

Table 13: Summary statistics for the estimates obtained with the MWaPP re-tracker in the part of the crossing close to the Newport tide and Hinkley tide gauge stations.

The results presented in Table 11 stand out among the others presented in this deliverable, as they have been computed based on a much lower amount of data points than the rest of the values presented here. The mouth of River Usk lies in a very complex scene with many manmade targets and an enclosed harbour area called Alexandra Docks. The Alexandra Docks is an enclosed harbour facility with still-standing water lying at 6m-8m higher elevation than the water in River Usk. This means that returned waveforms for the area where the track crosses the mouth of River Usk will be contaminated by strong signals occurring from within this dock area. This contamination sometimes results in the re-tracking algorithms estimating the water level heights systematically higher than the rest of the observed trend in the river. This phenomenon can be seen in Figures 28, 30, 32, and 34, where a red cluster of data in varying sizes and spread is placed above the height range observed in the open water area of the Severn Estuary, and apart from the other estimates within the Usk River. The different re-trackers all estimate this erroneous water height, but the MultiPTR re-tracker is especially vulnerable to contamination from this secondary water body as can be seen in Figure 30. The MultiPTR re-tracker is systematically incapable of correctly estimating the water heights within River Usk in the same fashion as it failed to correctly estimate the water heights within the Fos-Sur-Mer canal area. For the MultiPTR re-tracker, this means that no meaningful validation statistics could be computed for the results obtained using it, and for the rest of the re-trackers, it meant that only a very few numbers of valid data points are very available from within River Usk in the overlapping sensing periods.

The Correlation statistic seen in Table 11 is close to 1 for all the re-trackers that were capable of correctly estimating the water height within River Usk. This is in part due to the large variance in observed weather heights caused by the diurnal tides in the scene (range up to 15m) meaning that proportionally larger deviations between the estimated and observed data would be needed to decrease this value, and in part due to the small sample size on which the statistics were computed. The RMSE value obtained using the MWaPP re-tracker is the smallest among the obtained statistics, but the small range of available sample sizes for the different re-trackers makes meaningful comparisons difficult.

The data presented in Table 12 however has the same (albeit still small) sample size as was typical for the other study area. The RMSE value obtained from the MWaPP re-tracker is here again the smallest, with the PTR and MultiPTR re-trackers performing significantly worse than the other re-trackers. It should be noted however that the Weston-super-Mare micro-gauge is incapable of capturing the entire range of the diurnal tidal signal. The gauge is placed at the end of a pier where the water fully retreats during low tide, exposing the riverbed of the Severn Estuary. This is visible as horizontal line sections in magenta lines illustrated in Figures 29, 31, 33, 35, and 38. This of course means that a complete picture of the re-trackers abilities to follow the observed trend in the open water areas cannot be formed. The Correlation statistic in the table is likewise close to 1 for the same reason as in Table 11. While the MultiPTR re-tracker performs statistically worse than the MWaPP re-tracker, it does however have much cleaner data clustering in the open water area than all the other re-trackers. This might make the MultiPTR re-tracker better suited for estimating water surface heights in open water, and this possibility should be explored more in future work.

The results of the tide gauge validation presented in Table 13 show statistics comparable to the ones presented for the MWaPP in Tables 11 and 12 with a few notable differences. The median bias added to the different tide gauge measurements differs significantly, while the added ellipsoid offset is almost identical. This may be due to a local datum or instrument calibration error. The correlation statistic computed for the tide gauge validation test is identical to the one computed for many of the micro-gauge validation tests, but the RMSE cor. statistic is slightly worse for both tide gauges. These statistics have however been performed on a significantly higher number of sample points than any of the micro-gauge station tests, which means that they are likely to be a more realistic depiction of the true capabilities of the MWaPP re-tracker. The estimated and realigned observed trends in Figures 36 and 37 are all within a < 2m range of one another, so the trends are still in good agreement despite this increase in RMSE cor.

Time constraints meant that no posting rate validation could be performed for the Severn Estuary, but this would be a top priority in any future work.

With all these factors in mind, there is evidence to suggest that the MWaPP re-tracker would be the superior option when re-tracking a study area like the Severn Estuary.

6 Detection of small-scale physical signals (WP2300)

This section report on the investigation of work done on WP2300 on the detection of small-scale physical signals (surface gradients, currents, roughness signatures) in highly tidal regions and investigate the applicability of FF-SAR to detect and measure tidal asymmetry/gradients across estuaries not seen with conventional altimetry. We were limited to look at height related quantities (surface gradients, and currents) as we only used empirical re-trackers which do not solve for roughness signatures.

The secondary objectives were to extend the drone flights to support further analyses (for example) of discharge at river outflow points. However, logistical considerations limited the duration and timing of the drone flights so it was only possible to carry out flights to the closest satellite passes.

The prime objectives for the drone flights were to provide geo-referencing for the installed micro-gauges, and to link the water level at the location of the gauge to that of the nearest overpass. We have reported the comparison between drone and satellite observations in section 6.2 below.

It was noted that user agencies expressed high interest in further use of drones equipped with altimeters for future studies.

6.1 Tides in Severn

In this study we focused on the possibility to determine tidal asymmetry/gradients across the estuaries but also investigate if we can detect small-scale tidal signals in the Severn Estuary. We investigate if we can determine the full signal or alternatively, the residual ocean tide signal not mapped by the FES2014 ocean tide model.

When investigating tides in inlets like the Severn, the rotation of the Earth creates rotational patterns of the tides as illustrated in Figure 39 (right). This creates an asymmetry around a node in the estuary with high water to the south (low water to the north) at incoming or rising tides and vice versa on outgoing/falling tides. The Severn Estuary is famous for tidal resonance creating maximum tidal ranges at spring tide of around 14 metres. The Severn is far from a perfect inlet where the tides can rotate 360 degrees because the Severn is more like a complex funnel which seriously alters the rotational pattern. The right panel of Figure 39 illustrates the amplitude and phases for several tide gauges in the Severn as a function of their coordinates so it's possible to deduce how far up the Estuary the stations are situated. It can be seen that the phases only vary from 144 to 195 degrees for various tidal stations in the Severn Estuary. This means that we will only see a minor rotation and more ingoing/outgoing tides. We do however still expect to map some "rotational" signal or to be more correct a sloping surface that slopes up to the south at incoming/rising tides and up to the north at outgoing/falling rides.

Station	M2 Amp	M2 pha
	Obs.	Obs.
Stackpole Quay (51.63,4.85)	2.51	168
Mumbles (51.57,4)	3.18	171
Swansea (51.62,3.93)	3.19	173
Port Talbot (51.58,3.78)	3.13	173
Barry (51.4,3.28)	3.92	185
Steep Holm Island (51.33,3.1)	3.87	186
Cardiff (51.48,3.17)	4.01	191
Weston-Super-Mare (51.35,2.97)	3.95	181
Hinkley Point (51.2,3.13)	3.8	195
Minehead (51.2,3.47)	3.59	183
Porlock Bay (51.22,3.6)	3.42	179
Ilfracombe (51.2,4.12)	3.04	162
Appledore (51.05,4.18)	2.57	165
Port Isaac (50.58,4.82)	2.47	144

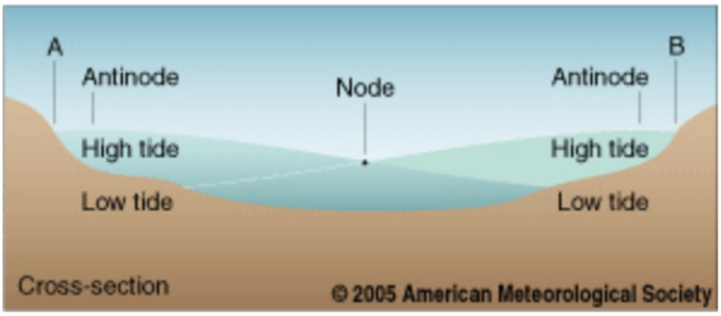

Figure 39. Left: Amplitude and phase at tide gauges in the Severn/Bay of Bristol as well as (right) illustration of the rotational a-symmetry of tides in a tidal inlet. Right Figure from: http://oceanmotion.org/html/background/tides-basins.htm

Following the result in the preceding sections, we decided to apply the MWaPP re-tracker at 1000 Hz. The reason for choosing MWaPP is that this re-tracker is based on a sub-waveform re-tracker but takes the shape of adjacent waveforms into account before selecting the sub-waveform belonging to the nadir. This proved to reduce snagging quite a bit. We used S3B RON 265 cycles 19 to 65 corresponding to a total of 46 cycles. These are illustrated in Figure 40 between Weston Super Mare on the southern side of the Severn and Newport on the northern side of the Estuary.

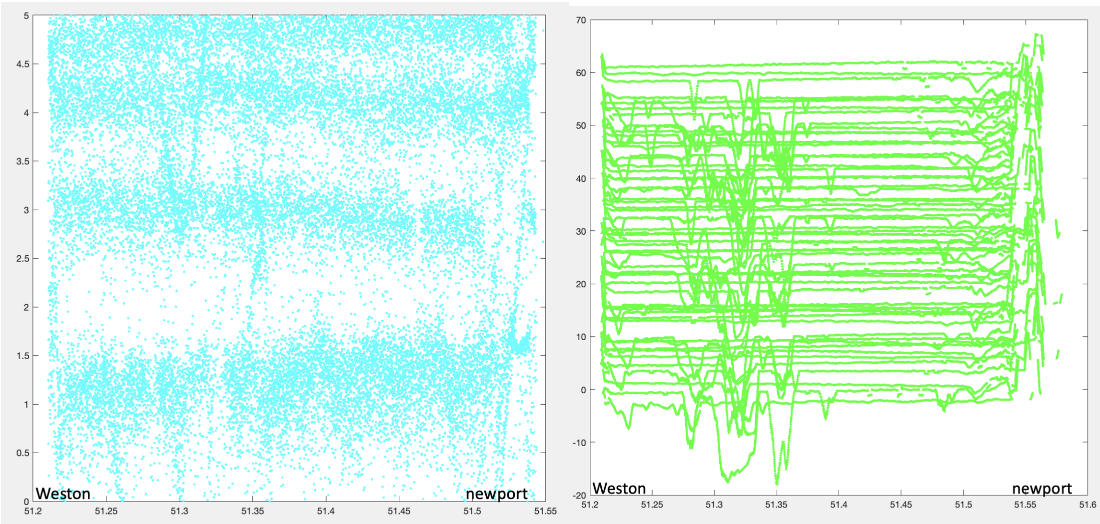

Figure 40. Left: raw 1000Hz retracted SLA relative to the DTU21 Mean sea surface. No tidal signal was removed. Only the first five cycles are shown. Right: Averaged 60 Hz data for all cycles.

The MWaPP re-tracked SLA at 1000 Hz relative to the DTU21MSS Mean sea surface is shown in Figure 40 with no tidal signal removed. The range precision is around 50 cm which is expected. Only the first five cycles have been shown.
The right panel in Figure 40 shows all 45 cycles of S3B track 254. A smoothing of 80 meters has been applied.

At these scales, a significant snagging is seen where the satellite snags to a location away from the nadir leading to a Sea surface height (ssh) drop of roughly 20 metres. Figure 40 shows the assumed cause for this in the Severn Estuary. Due to the huge tides, Newport, Cardiff, and Barry have tidal gates that seal the harbour at low tides so that ships can dock in the harbours. Consequently, they also explain why snagging is only seen during part of the tidal cycle when the tides are low and the gates are sealed causing still water in the harbours.

Figure 41. The expected causes for the snagging seen in the Sentinel-3B altimetry along track 254. The barracks at Newport, Cardiff, and Barry. The inserted picture is a zoom-in on Cardiff at low tides. The picture is from Google Earth.

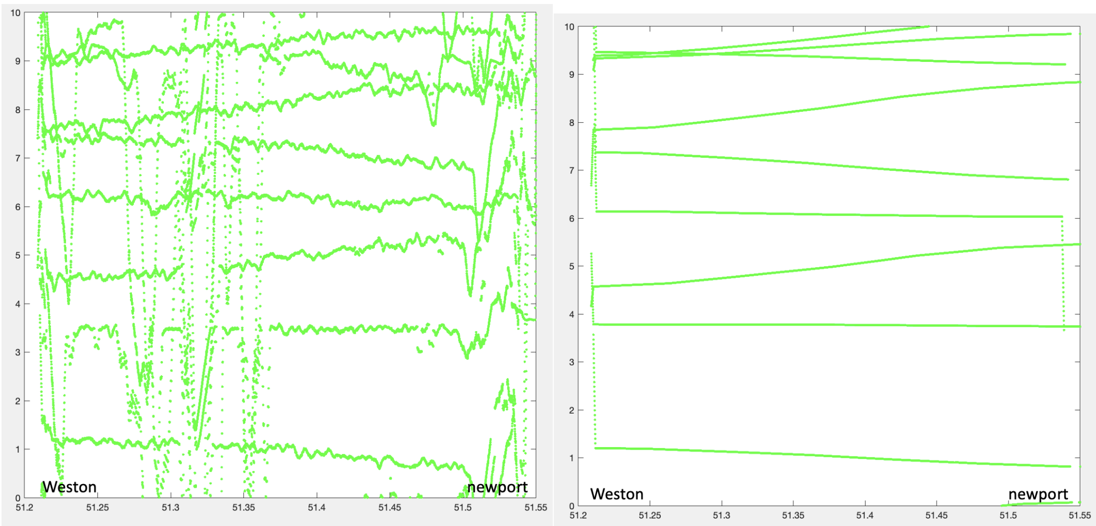

Figure 42 Left: Zoom of the sea surface height for the first seven cycles of S3B smoothed over 100 meters as well as the FES2014 ocean tide correction in the right panel.

Figure 42 illustrates the sea surface heights for the first 7 cycles. Despite some snagging, the tidal asymmetry is seen with variations in the slope of the sea level. The slope is validated against the FES2014 ocean tide model to the right.

The slope is as large as 1 meter over 30 km from Weston to Newport. Tides are shallow water waves, but we decided to use a geostrophic current approximation to determine if tidal currents could be mapped using such an approximation.
We found a slope of 1 meter of 30 km at incoming tides. This corresponds to a geostrophic current of around 2 meters perpendicular to the track. This is in surprisingly good agreement with the Severn Estuary partnership which presents measured tidal currents of 1.5 meters at incoming tides at Weston Super Mare.

Before performing a tidal analysis, it is important to check that the alias period is well-defined for Sentinel-3. It is well-known that the satellite is in sun-synchronous orbits which prevents the determination of several constituents. Fortunately, M2 is well-defined with an alias period of 230 days for S3A/B so it is relatively safe to predict using 3-4 years of Sentinel-3B. Consequently, we decided to determine this constituent along track 254.

	T/P+JA+S6 (9.916 days)	ERS, Envisat Saral (35 days)	S3A/B (27 days)	Cryosat-2 (368.239 days)
M_2	62	95	210	800
S_2	59	~	~	768
K_2	85	97	250	743
N_2	50	183	183	2095
K_1	173	365	365	1486
O_1	46	75	270	1262
P_1	89	365	365	1591
Q_1	69	133	232	5106
M_4	34	56	106	4633

Table 14: Alias period in days for various exact repeating satellites where the repeating period is given in the upper row.

We performed a tidal analysis for the well-defined M2 constituent from the 45 cycles of data (corresponding to 1200 days) along the track at 1000 Hz or 6 meters resolution to see if this could reveal small-scale tidal signatures. The result of this analysis is shown in Figure 43.

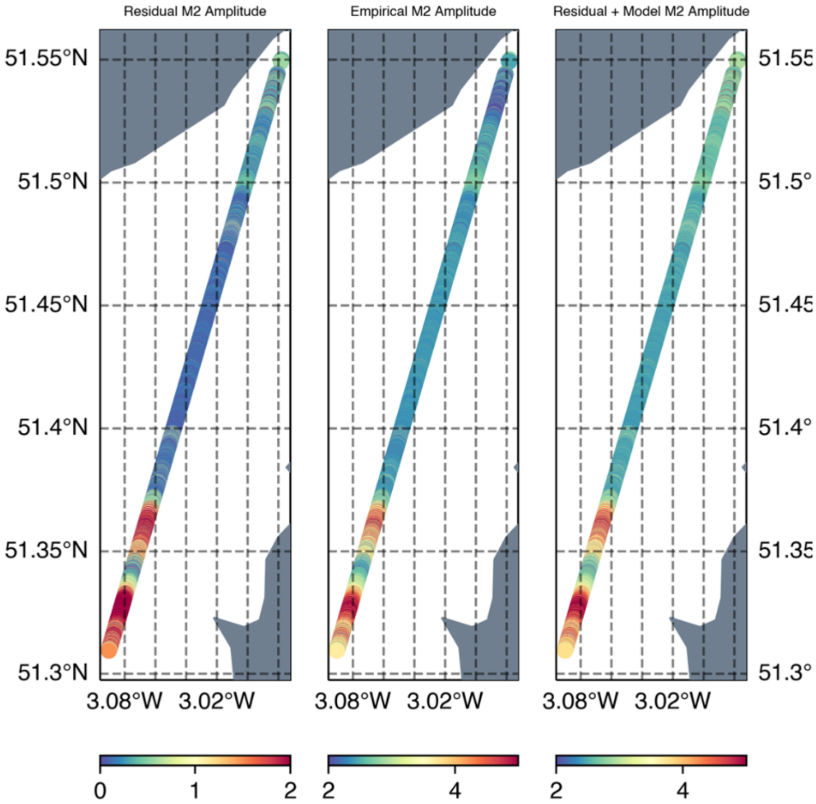

Figure 43. Left figure: Residual M2 tidal estimate (meters) to FES2014b along the transect from Weston to Newport. Central figure: Tidal estimate from the full sea surface height signal. Full tidal estimate (Residual + FES2014b)

The result in Figure 43 is very interesting in the sense that we do find significant tidal residuals to FES2014b ranging up to 1.6 meters for M2 along the track when using the 100 Hz sampling rate of 6 meters. This is particularly seen in the southern end of the track toward Weston Super Mare where the M2 tides are expected to be around 4 meters (Figure 43)

The FES2014b model is a finite-element model but given on 1/16 km resolution so it cannot resolve signals shorter than 12 km. The results show significant tidal variation on the 1 km scale in the southern part of the track some kilometres from Weston Super Mare. A closer inspection reveals that the tidal variations are highly correlated with the two islands called Flat Holm (https://en.wikipedia.org/wiki/Flat_Holm) and Split Rock located in the centre of the Estuary. Between the two islands, there is an opening that ranges between hundreds and meters at low tides and several kilometres at high tides. The water depth also varies from a few meters to 20 meters depending on the tidal height. We expect this variation in width and depth to be responsible for creating large variations in the tidal range close to the islands.

Within 5 km we find tidal residuals varying from 1.5 meters to 40 cm and back to 1.5 metres. Such large amplitude differences will create significant tidal currents which are not yet mapped using the state-of-the-art ocean tide model FES2014b. This is a very promising result as this is the first time we have been able to determine tides at such high spatial resolution from FF-SAR altimetry. The result is more impressive since they were determined in the presence of significant snagging causing very large sea level "noise".

The final two panels in Figure 40 illustrate an estimation of M2 tides independent of any tidal model. This was done in the central figure where we did not apply the FES2014 first but rather estimated the full tidal range. Estimation of the residual tides to FES2014 and adding this back compared very closely with our estimation of the full tidal signal which means that we have confidence in our findings. This can be seen by comparing the central figure and the right figure using the residual approach. It is scientifically very interesting that we can determine the FULL M2 tidal amplitude to an accuracy of around 10 cm for the investigated track.

Despite the very promising results, Sentinel 3 is still problematic for tidal modelling as the satellite is in a sun-synchronous orbit. It is likely questionable if many other tidal constituents can be retrieved from the data. With respect to retrieving tidal constituents from FFSAR it would make more sense to perform an investigation of data from Sentinel 6. The downside here is that this satellite does not have tracks inside the Bristol Channel.

We recommend that further S3A/B data are re-tracked and analysed to investigate and validate our findings for the M2 constituents as part of a scientific paper. Such extended analysis could also be designed to deal better with the very severe problem of snagging which was seen in many places and which is dependent on the magnitude of the tides when the tidal locks are in place in several locations. This is, however, outside the scope of this deliverable.

6.2 Slopes and currents

We looked at the surface slopes for both Severn and Rhone in a comparison with the Drone flight by vorteX.io.

Once the mean deviation from the geoid is computed, the surface geostrophic currents are associated with the slope of this surface. This requires that accelerations and friction terms are neglected and horizontal pressure gradients in the atmosphere are absent which we can safely assume in our regions.
However, we quickly encountered that the S3 profiles for both the Rhone river, the Rhone coast and the Severn have significant difficulties due to mainly snagging and tides, preventing a meaningful interpretation.

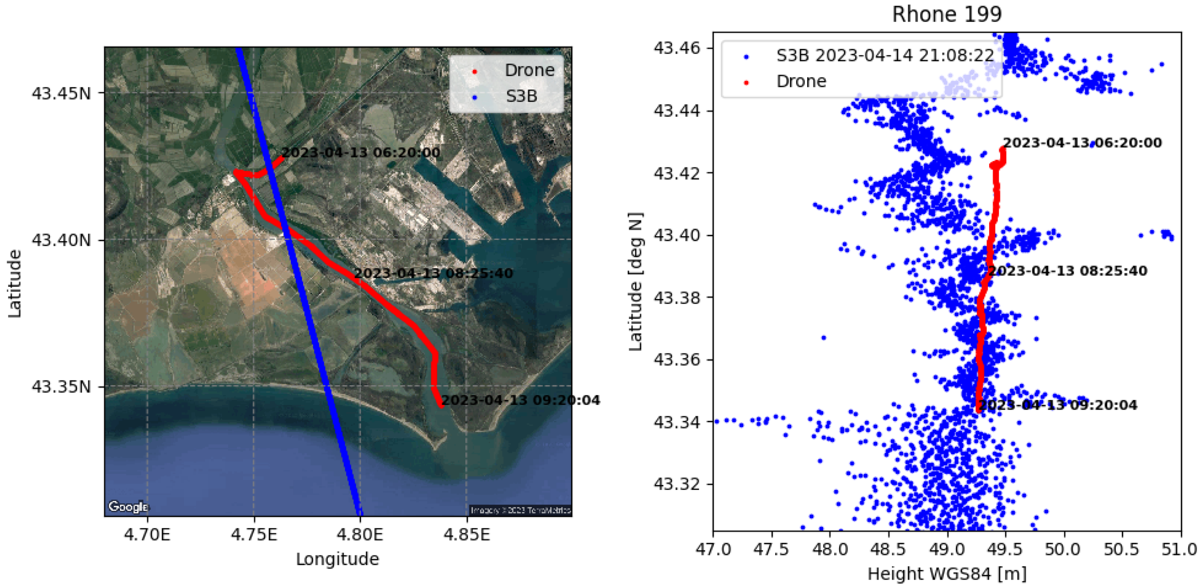

Figure 44. The river height from Sentinel 3B and the Drone height along the Rhone River. Severely snagging of the satellite is seen between 43.36 and 43.42 due to the inclination of the River with respect to the ground track.

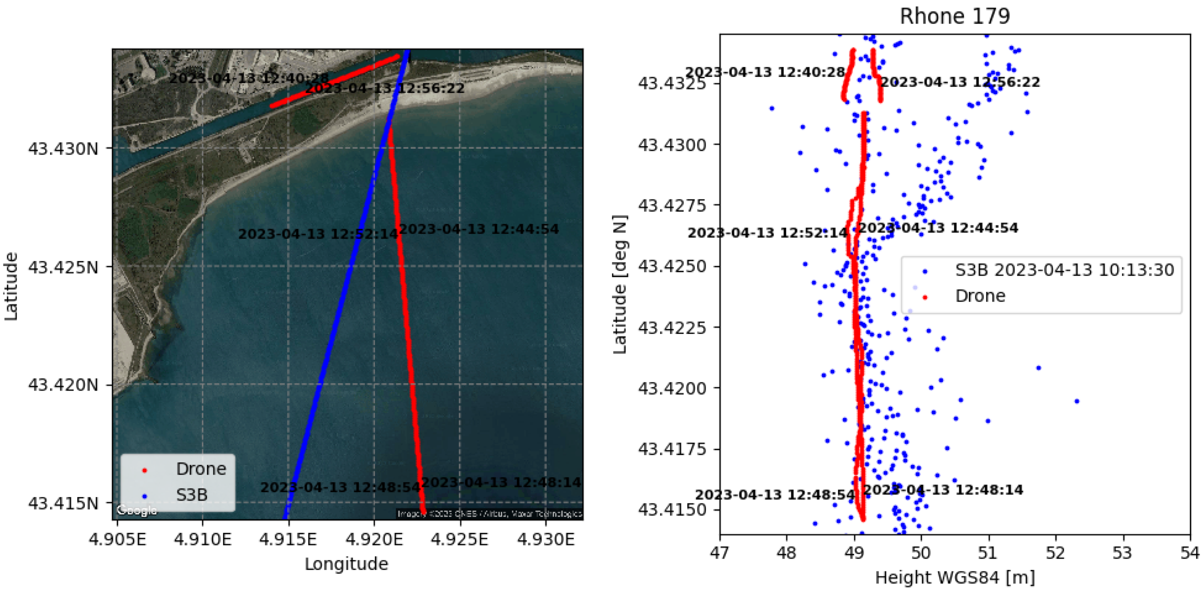

Figure 45. The sea surface height from Sentinel 3B and the Drone height offshore of the mount of the Rhône river. Severe snagging to an in-land canal is seen close to the coast and the different inclination of the drone flight and the satellite track is evident in the Mediterranean Sea.

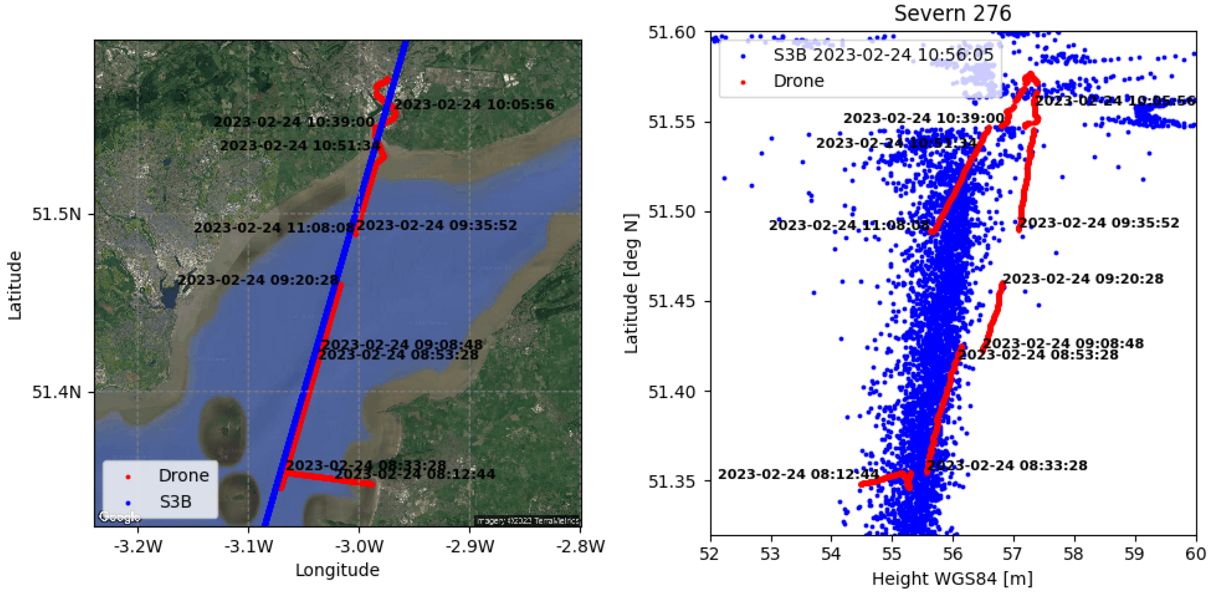

Figure 46. The height of Sentinel-3 and the Drone flight across the Severn. In the right panel we have added the exact times of the drone flight which is within 3 hours of the Satellite pass as the drone flies at a much lower speed.

The comparison between the water level data from the drone flights and Sentinel-3 is shown in Figures 44 to 46. The effect of severe snagging of the satellite data is seen in and around the Rhone river (figures 44 and 45) making it impossible to deduce information about the actual river slope for the current satellite pass.

For the Severn the tides are a limiting factor. Because the drone flies with limited speed it takes several hours to cross the Severn. The same crossing is done in a few seconds by the Sentinel-3 satellite. Because the tidal range typically changes by 8 metres in 6 hours, the drone water heights can be seen to diverge from S3B water heights in Figure 46 as the flight progresses. The S3B overpass was at 10:56 which is close to the time that the drone flight passed south of Newport (latitude 51.5N). High tide at Newport on that day (24 February 2023) was at 11:00 UTC.

7 Summary and Conclusions

In this study, we have evaluated the quality and benefits of the FFSAR data through comparison with the vorteX-io micro-gauges in the Rhône and Severn Estuaries. Additionally, we have tested different re-trackers, and parameter settings in the SMAP processor for the posting rate and the illumination time.

For track S3B-179 elevations were estimated using the MWaPP re-tracker for posting rates between 500Hz and 1500Hz in the narrow canal and validated against the micro-gauge. This was done with an illumination time of 2.3 s and 1 s. The statistics in terms of RMSE and correlation were similar with the two different illumination times. For this track, a posting rate of 700 Hz showed the best results with a corrected RMSE of 3 cm and a correlation of 0.96. On the downside, the relatively low posting rate resulted in fewer times with valid elevations. The RMSE and Correlation statistics for higher posting rates were slightly worse but offered better temporal data coverage. The posting rate test for track S3B-199 was evaluated for both the south and north crossing of the Rhône River. The statistics for all posting rates were very similar, and none of the posting rates offered a substantial benefit over another. Based on this limited evaluation, a higher posting rate is recommended when observing small and or narrow targets.

Four different re-trackers were tested, the PTR, Multi-PTR, the OCOG re-trackers build into the SMAP application and the standalone MWaPP. In general, the MWaPP re-tracker had the best performance when compared to the micro-gauge reference data. The Multi-PTR re-tracker was systematically incapable of correctly estimating the water surface level height in narrow water bodies but performed relatively well over open water bodies and in homogenous scenes. The MultiPTR re-tracker may have additional benefits when re-tracking large open water bodies in the size of the open water bodies in the Severn Estuary, but a deeper analysis would be needed to test this hypothesis. It must be stressed here that the overlapping sensing periods between the gauge and the altimetry data are very short, in fact well below one year.

The validation test performed for the MWaPP re-tracker using the UK tide gauges provide further evidence for the ability of the MWaPP re-tracker in providing accurate water level heights in the Severn Estuary. The time series for the estimated and realigned observed time water heights follow each other with a good degree of accuracy for the entirety of the multiple-year time span in which they overlap. The validation based on the water heights observed by the Hinkley tide gauge provides less clear results, but assuming that the deviations between the estimated and realigned observed trend were caused by instrumentation error, there is some evidence that the MWaPP may likewise be capable of accurately estimating the water heights in the open water near the Hinkley tide gauge. A larger validation study is however needed to conclude definitively which re-tracker may be best suited when estimating water heights in shallow or coastal waters.

The largest benefit to be gained using FFSAR-based elevations instead of the standard 20Hz OCOG elevations is the increased accuracy and data coverage over small targets e.g. the manmade canal in Fos-Sur-Mer, and the mouth of River Usk in the Severn Estuary. The 20Hz OCOG re-tracker was only able to observe the canal in Fos-Sur-Mer at a few dispersed points in time, and it was therefore not possible to evaluate the quality of this re-tracker for that scene. For the Severn Estuary, the quality of the 20 Hz OCOG data is comparable to those obtained using FFSAR processing. However, the FFSAR data provided more detailed information about the surface water slope, especially at the mouth of River Usk.

Based on the analysis carried out here, we find that the use of FFSAR processing is highly beneficial when observing small targets, water slopes, and near coastal areas.

As this study only included a few sites that in addition are very different in terms of the water level variations, it would be beneficial to test and evaluate the use of FFSAR-based sea levels at more coastal sites and water levels at additional river sites to get a more solid understanding of the benefits of FFSAR.

The Severn Estuary tidal study from FFSAR revealed the ability to determine tides at kilometre spatial resolution from FF-SAR altimetry. These results are novel and interesting in the sense that we do find significant tidal residuals of up to 1.6 meters for M2 along the track at the sampling rate of 6 meters relative to the state-of-the-art Ocean tide model FES2016b. This is particularly seen in the southern end of the track toward Weston Super Mare. The significant tidal variation on the 1 km scale in the southern part of the track is associated with the two islands called Flat Holm and Split Rock located in the centre of the Estuary.

8 References

[Egido, A., & Smith, W. H. (2016). Fully focused SAR altimetry: theory and applications. IEEE Transactions on Geoscience and Remote Sensing, 55(1), 392-406.] (https://ieeexplore.ieee.org/abstract/document/7579570)

[Guccione, P.; Scagliola, M.; Giudici, D. 2D Frequency Domain Fully Focused SAR Processing for High PRF Radar Altimeters. Remote Sens. 2018, 10, 1943.] (https://doi.org/10.3390/rs10121943)

[Shaw. A., (2023), "Impact Assessment Report on the Bristol Channel and Severn Estuary", Internal Project Case Study Report for ESA HYDROCOASTAL Project, June 2023.]

[Villadsen, H., Deng, X., Andersen, O.B., Stenseng, L., Nielsen, K. and Knudsen, P., 2016. Improved inland water levels from SAR altimetry using novel empirical and physical retrackers. Journal of Hydrology, 537, pp.234-247.] https://doi.org/10.1016/j.jhydrol.2016.03.051

9 List of Acronyms

AD	Applicable Documents
CCO	Channel Coastal Observatory
DTU	Danmarks Tekniske Universitet (Technical University of Denmark)
EO	Earth Observation
ESA	European Space Agency
MTR	Mid Term Review
NOC	National Oceanography Centre
RD	Reference Document
RON	Relative Orbit Number
SAR	Synthetic Aperture Radar
SatOC	Satellite Oceanographic Consultants Ltd
SMAP	Stand Alone Multi-Mission Processor
SRAL	SAR Radar Altimeter
S3A, S3B	Sentinel 3A, and Sentinel 3B

Annex 1: Validation of vortex.io microgauge data against other gauge data: Newport and Weston Super Mare

Authors: Dougal Lichtman, Simon Williams, Paul Bell (National Oceanography Centre, UK), David Cotton (Satellite Oceanographic Consultants, Ltd)

1. Summary

NOC have carried out a comparison of water level measurements from the vortex.io microgauges installed on the Severn Estuary, UK, at Newport and Weston Super Mare, to other gauges located close to these two gauges.

Comparing the Vortex-io water level measurements against those from a GNSS-IR (Weston Super Mare) and a standard bubbler system (Newport), showed close agreement at both locations (gradient close to 1.0), but with biases. The biases are thought to be due to errors in the levelling of the Vortex-io stations, as both the GNSS-IR and bubbler gauges have traceable levelling data. A comparison of the tide gauge water levels at Newport to local river levels suggests that these gauges are affected by river flow.

2. Introduction

For the FFSAR project, two Vortex-io water level gauges were deployed, one on a road bridge near Newport in Wales and the other on the pier at Weston Super Mare (Figure 1), both installed on 6th September 2022. In this report we compare the data from the Vortex-io gauges to a conventional bubbler tide gauge and a GNSS-IR system.

The Vortex-io is a water level gauge based on a laser altimeter. The instruments deployed for the FFSAR Coastal project are set up to take measurements every thirty minutes, each measurement period lasts 30 seconds which corresponds to 210 LiDAR pulses. The median is taken of the 210 pulses. Both the Newport and Weston Gauges Vortex-io (Figure 1) were levelled through a drone survey referenced against a GNSS base station.

For both Vortex-io gauges, the measurement time was set to match the time of the Sentinel 3B satellite overflight. The first vortex.io gauge installed at Weston Super Mare began to display problems in March and the sampling became random. It failed on March 10th, but there were irregularities before then, and it was replaced on April 6th.

To validate the Vortex-io data, data from a GNSS-IR system was used for the Weston Pier site and from the Natural Resources Wales tide station at Newport. The Newport system is a pneumatic bubbler with two full-tide and mid-tide measuring systems, sampling every 15 minutes, levelled to Ordnance Survey auxiliary benchmarks (National Tidal & Sea Level Facility, https://ntslf.org/tgi/portinfo?port=Newport). At Weston the GNSS-IR water level gauge is a system built by the National Oceanography Centre, deployed as part of the SWOT-UK project. The system was

levelled using the GNSS data and has an irregular sample interval to coincide with the pass times of the SWOT satellite. As the GNSS-IR system collects dual frequency measurements, the antenna height can be measured to the International Terrestrial Reference System and Frame, and therefore height above the ellipsoid.
The intertidal flats dry out at low water by Weston Pier and then bed level is measured by the Vortex-io and GNSS-IR systems. At the Newport Vortex-io site, the river levels are measured once the tide goes out.

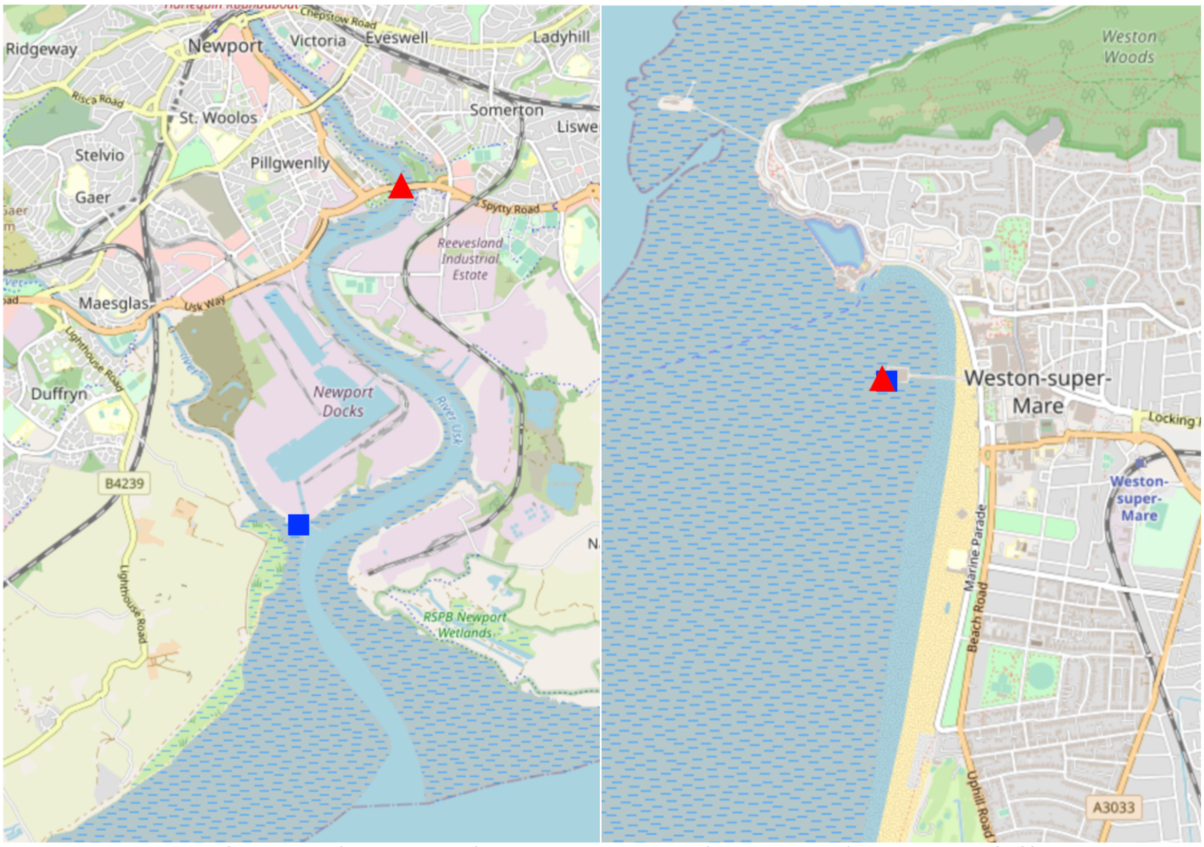

Figure 1: Locations of vortex.io (red triangles) and nearby gauges (blue squares) at Newport (left) and Weston Super Mare (right)

3. Method

Initially the raw GNSS-IR data had noise removed for above the high-water limit and below the seabed level. The data were split into blocks by finding gaps in the times of the data greater than five minutes. The blocks were then filtered using a median to a single value not biased by extreme outliers. As the GNSS-IR system had a higher sampling rate, the data were interpolated to the times of the Vortex-io using a modified Akima function. The Akima function represents both the sinusoidal and flat sections of the data better than Spline or PCHIP (Piecewise Cubic Hermite Interpolating

Polynomial) functions. Finally, the data were corrected for the median of the antenna height (nominal antenna phase centre).
The bubbler data were interpolated to the times of the Vortex-io using a modified Akima function. No further processing was required.

4. Results

1. Newport

Although the gauges at Newport are not collocated, there is good agreement (Figure 2 and Figure 4). The level of the river can be seen where the Vortex-io data are cut off compared to the bubbler gauge (Figure 2 and Figure 3). Comparing gauge water levels (Figure 2) with water levels at Usk approximately 20 km upriver (Figure 3), in particular in January, suggests that the bubbler gauge may also be affected by the river levels. The data in Figure 4 show a clear linear relationship and excluding the data below 48 m gives a regression slope of 0.99 and intercept of 0.19 (no. obs. = 7234, R2 = 0.985, F-stat = 4.77e+05, p-value = 0).

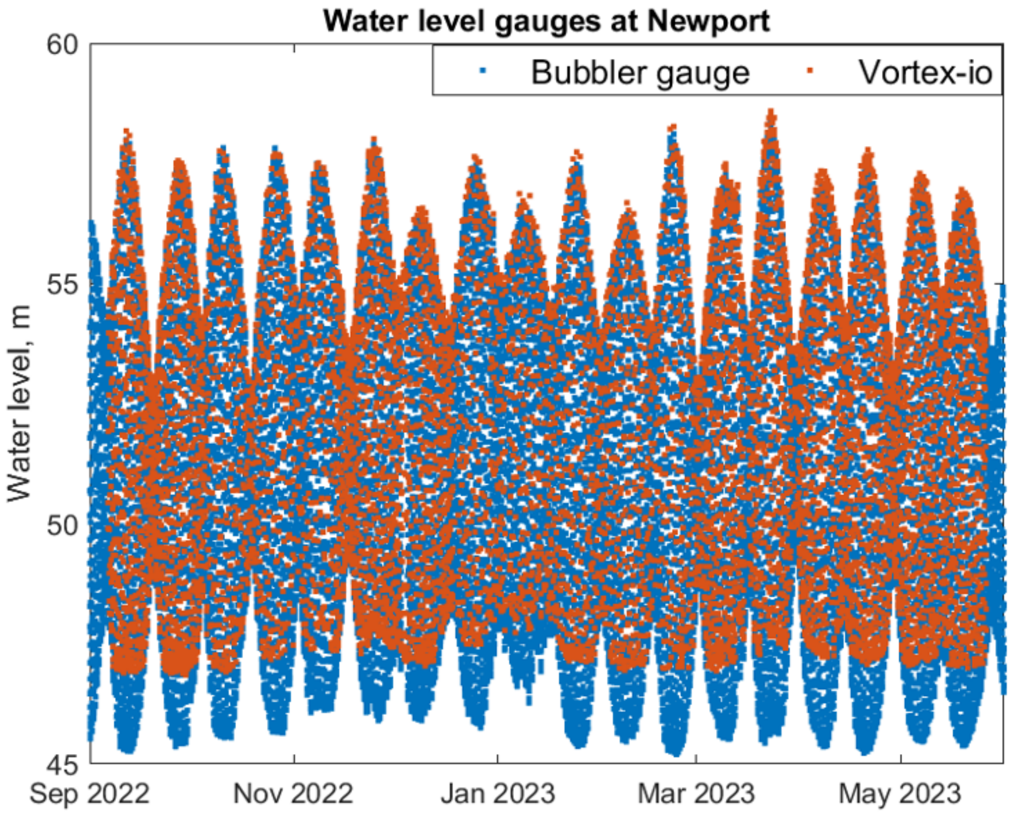

Figure 2: Time series of water level gauges at Newport. Bubbler gauge at Newport Harbour entrance (blue dots) and vortex.io micro-gauge on Newport Road bridge (red dots).

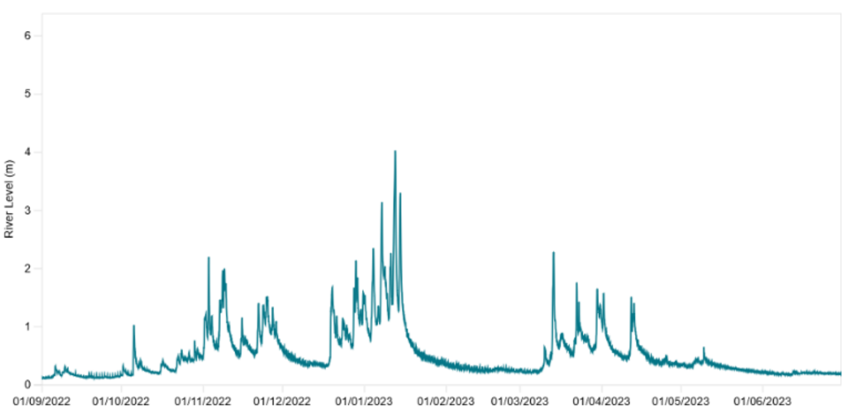

Figure 3: River levels for the Usk at Usk Town. (https://rivers-and-seas.naturalresources.wales/Station/4054?parameterType=1).

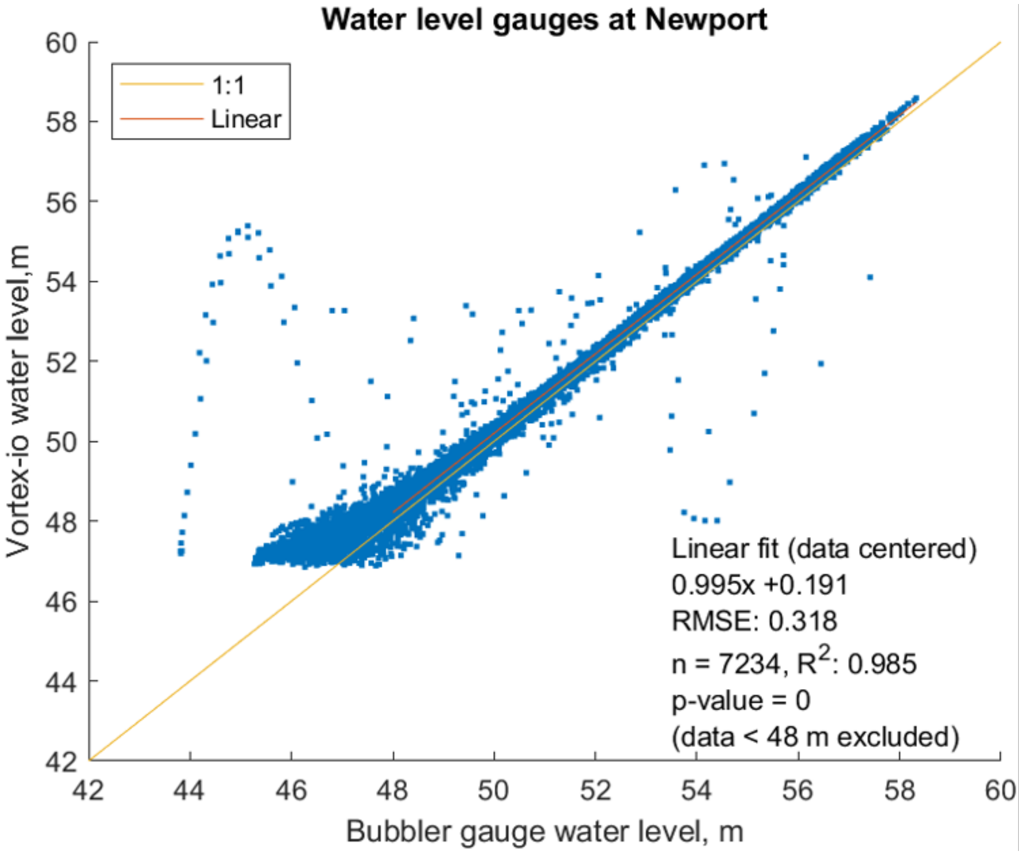

Figure 4: Comparison of Bubbler gauge and Vortex-io water levels at Newport. Yellow line – 1:1 line. Red line – linear regression fit (data centred).

2. Weston Super Mare Grand Pier

The data at Weston pier are notably offset (Figure 5), though they show the same trend with both systems measuring the seabed at low tide. The data show a clear linear relationship (Figure 6), with a regression slope of 1.06 and intercept of 1.11 (no. obs. = 2449, R2 = 0.984, F-stat = 1.5e+05, p-value = 0).

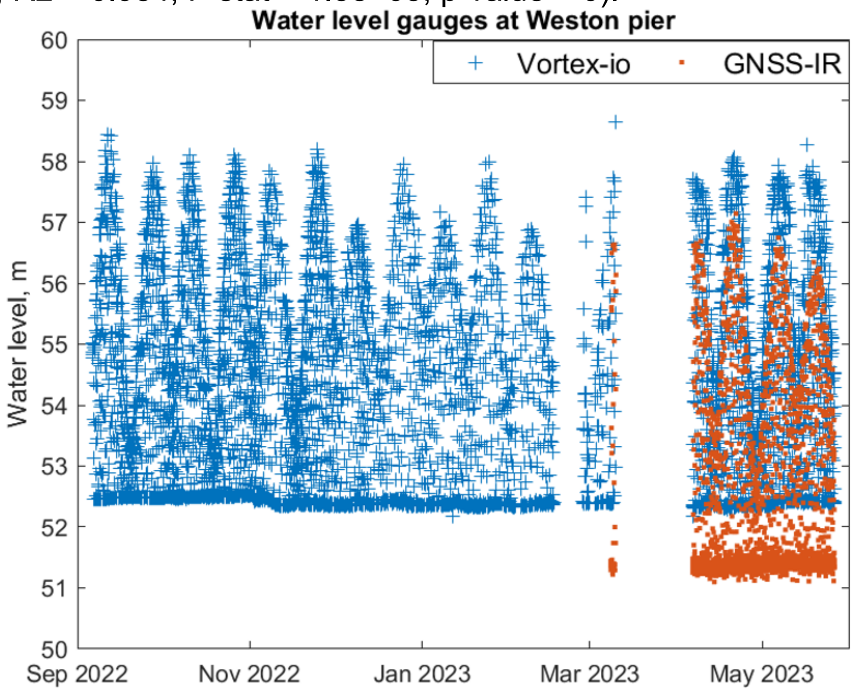

Figure 5: Time series of water level gauges at Weston Super Mare Grand Pier. GNSS-IR data are indicated by blue crosses and vortex.io micro-gauge data by red squares.

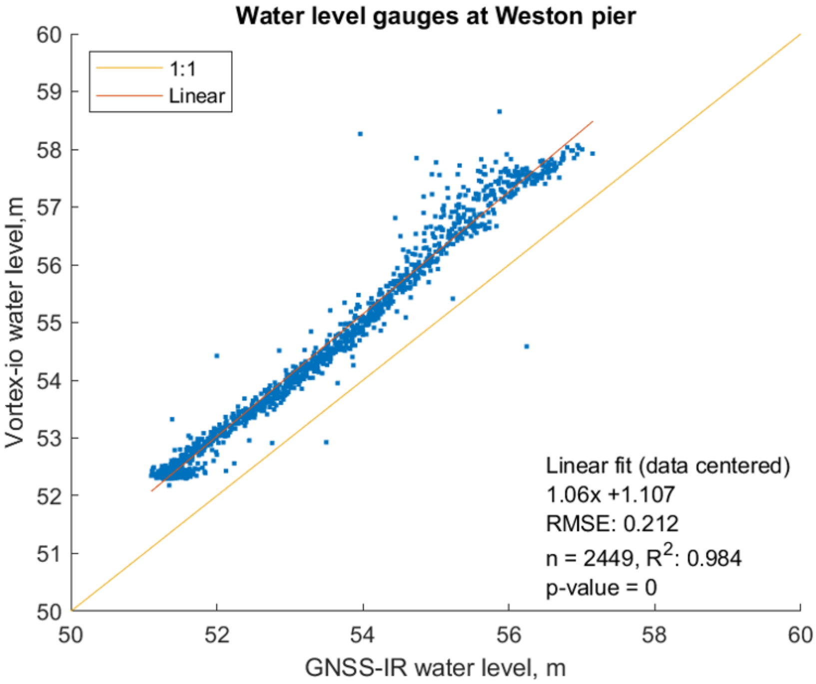

Figure 6: Comparison of GNSS-IR and Vortex-io water levels at Weston Pier Yellow line – 1:1 line. Red line – linear regression fit (data centred).

5. Conclusions

The Vortex-io water level measurements agree well with the GNSS-IR and standard bubbler tide gauges, the trends are close to one to one but with an offset. The offsets were probably due to the levelling of the Vortex-io stations, as both the GNSS-IR and bubbler gauges have traceable levelling data. Comparing the tide gauges at Newport to local river levels, suggests that these gauges are affected by river flow.

Annex 2: Comparison between the vortex.io drone measurement and the NTSLF gauge at Newport

Author: David Cotton (Satellite Oceanographic Consultants, Ltd)

1. Summary

The water level measured by the vortex.io drone is compared to the measurement from the Newport NTSLF gauge at the time of the drone point of closest approach to the gauge. The drone measured water level was 57.206m above WGS84, the gauge measurement was 18.5cm higher, at 57.391m

2. Introduction

On 28 February, vortex.io managed a drone campaign over the Severn Estuary in UK. The prime objective was to provide a geo-reference level for the vortex.io microgauges installed at Newport and Weston Super Mare for the FFSAR project, and to provide a continuous water level measurement between these gauges and the nearest ground track of Sentinel 3B at these locations, as close to the time of the overpass as possible. Full details of the drone campaign are available in FFSAR Deliverable 3.1 (In Situ Data Campaign Report)
This note reports on a cross validation carried out by SatOC between the vortex.io drone measurement and the NTSLF Tide Gauge at the entrance to Newport Harbour

3. Method

During its flight on 28 February 2023, the vortex drone held a stationery location close to the entrance to Newport harbour at an altitude of 15m for 1 minute centred at 10:00 GMT (Figure 1, left Panel). The geo-referenced water level measured by the drone was extracted from the smoothed data set for that period (figure 1, right panel). The mean water level measured by the drone for the 30s period centred on 10:00 GMT was 57.206m above WGS84, the value at 10:00 was 57.202m.
The value recorded by the Newport harbour bubbler gauge at 10:00 was 6.745m above ordnance datum, corrected, or 57.384m with respect to WGS84. So, the Newport NTSLF bubbler gauge is giving a water level 17.2 cm higher than the drone.

The reason for the 17.2 cm difference is not clear without further analysis. The drone data show a gradient in water level along the Usk River, but this is not expected to be of the order of 17.2 cm over a separation of 205 m.

Figure A1 Left – drone flight trajectory and location of 1 minute hover at entrance to the Newport Harbour. Right - The NTSLF bubbler gauge is located on the western harbour pier (left) at the end of the yellow line, close to the lock gate. The NTSLF gauge is estimated to be 205m from the drone location.

Figure A2 Drone water level time series around 10:00 GMT 28 February 2023.